Key Words: Plutonium, oxidation state, pH, soil, sediment

Retention: Permanent

Plutonium Oxidation State Geochemistry in the SRS Subsurface Environment (U)

Brian A. Powell[(a)], Robert A. Fjeld[(a)], and John T. Coates[(a)], Daniel I. Kaplan[(b)], and Steve M. Serkiz[(b)]

[(a)] Clemson University
[(b)] Westinghouse Savannah River Company

December 27, 2002

Westinghouse Savannah River Company, LLC
Savannah River Site
Aiken, SC 29808

Prepared for the U.S. Department of Energy under Contract No. DE-AC09-96SR18500

Key Words: Plutonium, oxidation state, pH, soil, sediment

Retention: Permanent

Plutonium Oxidation State Geochemistry in the SRS Subsurface Environment (U)

Brian A. Powell[(a)], Robert A. Fjeld[(a)], and John T. Coates[(a)], Daniel I. Kaplan[(b)], and Steve M. Serkiz[(b)]

[(a)] Clemson University
[(b)] Westinghouse Savannah River Company

December 27, 2002

Westinghouse Savannah River Company, LLC
Savannah River Site
Aiken, SC 29808

Prepared for the U.S. Department of Energy under Contract No. DE-AC09-96SR18500

THIS PAGE INTENTIONALLY LEFT BLANK

TABLE OF CONTENTS

LIST OF TABLES

LIST OF FIGURES

LIST OF APPENDIX TABLES

LIST OF APPENDIX FIGURES

1.0 EXECUTIVE SUMMARY

The environmental mobility of plutonium (Pu) is profoundly influenced by its oxidation state. Pu(IV) is 2 to 3 orders of magnitude slower moving than Pu(V) or Pu(VI). For performance and risk assessment calculations, Pu waste has been assumed to exist in the less mobile reduced form, Pu(IV). Recent work on the chemistry of PuO_2 by Haschke and others (2000) has shown that PuO_2 may not be as thermodynamically stable as had previously been understood. Rather, some of the PuO_2 surface is oxidized in the presence of water, forming as much as 27% Pu(VI). This has significant implications to existing SRS programs (including the Pu Immobilization, LLW Disposal, and Remediation of the Old Burial Ground) and future SRS programs (including MOX and pit disassembly). Aspects of these implications are captured in the SRS Technology Needs/Opportunity Statement SR00-1026, "Reduce the Conservatism and Technical Uncertainty Associated with the Use of Literature Coefficients (K_d) to Describe Radionuclide Sorption to Sediments in PA Modeling."

The hypothesis of this Strategic Research and Development study was that even if Pu(VI) is produced in the waste form as suggested by Haschke and others (2000), it will be quickly reduced to Pu(IV) in the SRS subsurface environment. The overall objective of the research was to test this hypothesis through laboratory and computational studies conducted by Savannah River Technology Center and Clemson University scientist.

Dynamic flow experiments indicated that Pu(V) was very mobile in SRS sediments. As the pH increased, the degree of mobility and the fraction of Pu that became "irreversibly sorbed" to the sediment increased, albeit, only slightly. Conversely, these column experiments showed that Pu(IV) was essentially immobile and was largely "irreversibly sorbed" to the sediment. More than 100 batch sorption experiments were conducted with four end-member sediments, i.e., sediments that include the likely extreme chemical, textural, and mineralogical properties likely to exist in the SRS that will likely have an influence on Pu sorption. These tests were conducted as a function of Pu oxidation state, pH, and contact time. These results repeatedly showed that although Pu(V) sorbed initially quite weakly to sediments, it slowly, over the course of only 33 days, sorbed very strongly to sediments, to nearly the same degree as Pu(IV). This indirectly confirms our hypothesis that Pu(V) may in fact convert to the more strongly sorbing form of Pu, Pu(IV). This finding has very large implications for how SRS deals with the potential risk imposed by Pu entering our subsurface environment. It strongly suggests that once Pu enters our subsurface environment, even if it enters in the more mobile oxidized form proposed by Haschke and others (2000), it will likely have very low mobility, minimizing risk associated with long distance subsurface aqueous phase transport.

2.0 INTRODUCTION

The mobility of plutonium has significant implications for several existing (Pu Immobilization, LLW Disposal, and Remediation of the Old Burial Ground) and future (MOX and pit disassembly) programs at the Savannah River Site (SRS). The mobility of plutonium is highly dependant on oxidation state. Aqueous tetravalent plutonium, Pu(IV),exhibits a mobility 2 or 3 orders of magnitude lower than Pu(V) or Pu(VI). Reported Kd values (distribution coefficient, plutonium soil to water concentration ratio) for various plutonium oxidation states range from 10 to 10,000 mL/g (Prout, 1959). Transport models for the SRS subsurface assume that plutonium is stable as $Pu(IV)O_2$, which is a very insoluble crystalline material ($pK_{sp} \cong -56$) (Neck and Kim, 2001), exhibiting extremely low mobility.

However, research by Haschke et al. (2001, 2002) at Los Alamos National Laboratory indicated that up to 27% of the Pu on the surface of a PuO_2 solid was present in an oxidized form in the presence of water. X-Ray Photoelectron Spectroscopy (XPS) analyses indicated the plutonium was present as Pu(VI) (Haschke et al., 2001) and Extended X-Ray Absorption Fine Structure (EXAFS) spectroscopy analyses indicated that plutonium was present as Pu(V) (Haschke et al., 2002). It is possible that these observed variations are due to instrumental techniques (i.e., XPS is preformed under vacuum resulting in a lack of oxygen). In either case, the presence of oxidized forms of plutonium in plutonium solids raises questions concerning the assumption that plutonium in SRS sediments is present only as the low mobility, tetravalent form. Further analysis of the transport of plutonium in various oxidation states is therefore necessary.

Plutonium transport was found not to exhibit classical behavior in SRS sediment, even under relatively simple conditions (low carbonate aqueous phase with no potential ligands) (Serkiz et al., 2003). Experiments were preformed with a 250-420 μm fraction of SRS plutonium burial ground sediment. Plutonium fractions of different mobilities were observed at all pH values studied (3, 5, and 8). There typically were high, medium, and low mobility fractions in the column effluent. These data indicated that the plutonium in the column effluent after a Pu(V) spike remained as Pu(V). However, Pu(V) recovery decreased with increasing pH. This indicated that some Pu(V) was being retained, possibly irreversibly, on the column at higher pH values.

The conceptual model developed by Serkiz et al. (2003) and Fjeld et al. (2003) indicates that any plutonium that is oxidized within the SRS subsurface will be rapidly reduced to Pu(IV), therefore confirming the risk assessment assumptions already made. The conceptual model consists of three reactions:

a.) equilibrium partitioning of Pu(V) between the solid and aqueous phase,
b.) surface mediated reduction of Pu(V) to Pu(IV), and
c.) equilibrium partitioning of Pu(IV) between the solid and aqueous phase.

For this conceptual model, parameters reflecting the mobilities of both Pu(V) and Pu(IV) in SRS sediment are necessary for accurate modeling.

2.1 PLUTONIUM GEOCHEMISTRY

Interpretation of data pertaining to plutonium geochemistry is subject to a number of constraints due to the complex chemistry involved. The dominant reactions governing the fate and mobility of plutonium in the environment are oxidation/reduction, precipitation/solubility, complexation/hydrolysis and sorption/desorption. All of these possible reactions must be considered when attempting to define interactions between plutonium and natural materials.

2.1.1 Redox Chemistry

The chemical behavior of plutonium and other transuranic species in the environment is primarily defined by oxidation state. Due to variations of the chemical properties for each oxidation state, the reactions within the conceptual model must be considered with respect to each oxidation state. Plutonium is able to exist in five different oxidation states as the oxy/hydroxy ions $Pu(III)^{3+}$, $Pu(IV)^{4+}$, $Pu(V)O_2^{+}$, $Pu(VI)O_2^{2+}$, and $Pu(VII)O_4^{-1}$ (Cleveland, 1979). PuO_4^{-} is not considered a stsable species in the natural environment. In moderate pH or oxic groundwater, Pu(III) is readily oxidized to Pu(IV) (Choppin, 1997). For example, Pu^{3+} is rapidly oxidized by water at near neutral pH levels (Farr, 2000). This is due to the negative potential of Pu(III) at higher pH's. The standard reduction potentials for pH 0 and pH 14 are shown in Table 1. Therefore, the primary oxidation states of relevance in natural environments are Pu(IV), Pu(V), and Pu(VI).

Table 1. Standard reduction potentials (volts) of plutonium at pH 0 and 14 (Choppin, 1983; Allard et al., 1980)

Couple	pH = 0	pH = 14
Pu(III)/Pu(IV)	+0.982	-1.04 ± 0.24
Pu(IV)/Pu(V)	+0.170	+0.52 ± 0.24
Pu(V)/Pu(VI)	+0.916	+0.16 ± 0.24
Pu(IV)/Pu(VI)	+1.043	+0.34 ± 0.12

Oxidation state can also be influenced by disproportionation reactions where a single species serves as both the oxidizing and reducing agent. For example, a solution containing Pu(V) at a high enough concentration can disproportionate into Pu(IV) and Pu(VI). These concentrations are typically not encountered in natural systems (Choppin 1997). The extent of disproportionation reactions (equation 1) is also less likely in acidic solutions.

$$2Pu(V)O_2^{+} + 4H^{+} \Leftrightarrow Pu(VI)O_2^{2+} + Pu(IV)^{4+} + 2H_2O \qquad (1)$$

This is due to the fourth power dependence on the hydrogen ion concentration (Equation 2).

$$K = \frac{[Pu(VI)][Pu(IV)]}{[Pu(V)]^2[H^+]^4} \quad (2)$$

There is also a dependence on the square of the $Pu(V)O_2^+$ concentration, which is the reason higher concentrations (10^{-6} *M*) of Pu(V) are required for disproportionation reactions to occur in significant amounts.

Radiolysis of water can generate redox reagent, such as H_2, O_2 and H_2O_2, as well as short lived H, OH, and O radicals. These agents can react directly with plutonium or react with the sorbing phase in a system (Hobart, 1990). Reactions with the sorbing phase could be such that the oxidation state of plutonium is affected (Hobart, 1990).

2.1.2 Complexation and Hydrolysis

Complexation with available ligands can have a significant impact on the sorption of plutonium to surfaces by affecting the species charge and free energy of the molecule. The general affinity for complexation decreases with decreasing effective charge for each oxidation state in the following order (Choppin, 1983; Kim, 1986):

$$\underset{+4.0}{Pu(IV)^{4+}} > \underset{+3.2}{Pu(VI)O_2^{2+}} > \underset{+3.0}{Pu(III)^{3+}} > \underset{+2.2}{Pu(V)O_2^{+}}$$

where the effective charge is noted below each species (Choppin, 1983). The greater effective charge of PuO_2^{2+} compared to Pu^{3+} is due to the exposure of the equatorial side of the linear O-Pu-O^{2+} molecule (Kim, 1986). The general trend in the strength of the complexed species for actinides and various groundwater ligands is (Silva and Nitsche, 1995):

$$OH^- \geq CO_3^{2-} > F^- > HPO_4^{-2} > SO_4^{2-} > Cl^- > NO_3^-.$$

Hydrolysis dominates most complexation reactions for plutonium (further discussed below). Figure 1 shows an Eh-pH diagram for plutonium in 3.6×10^{-3} *M* HCO_3^-. The modeling was preformed using Geochemist Workbench® with the Lawrence Livermore National Laboratory's thermodynamic database (Delany and Lundeen, 1990). Carbonate dominates the speciation for Pu(VI) at pH values greater than about two and Eh greater than 0.5eV. Trivalent and pentavalent plutonium are primarily present as free ions. $Pu(OH)_4$ is dominant Pu(IV) species.

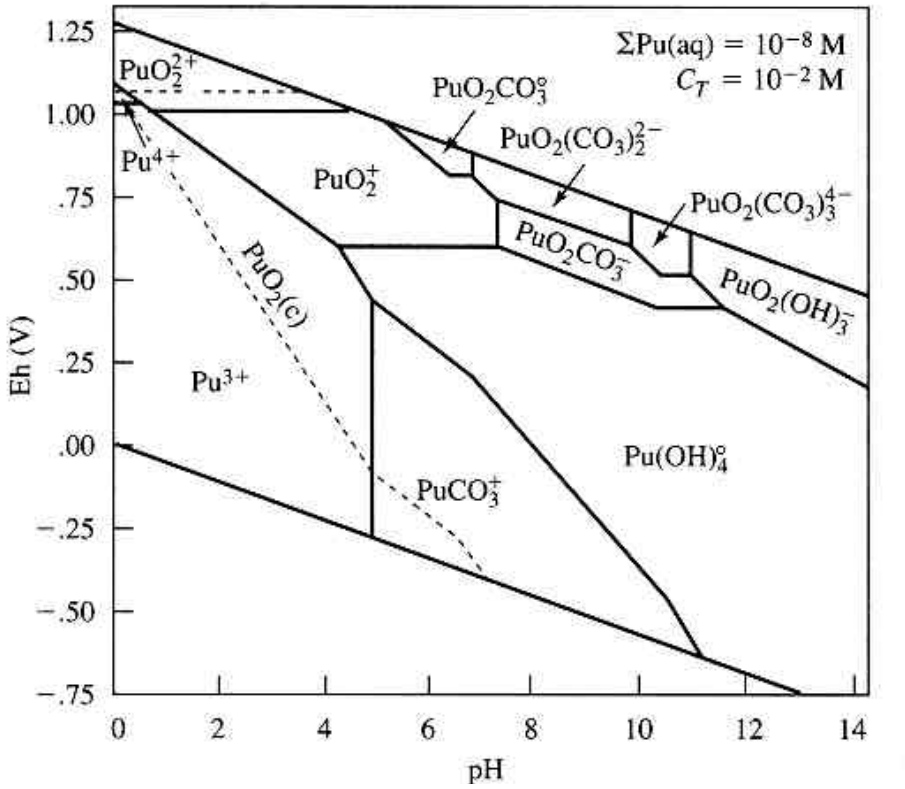

Figure 1. Eh-pH diagram of the plutonium-carbonate system at 25°C and 1 bar pressure. Dashed lines indicate the stability field of PuO_2(s) Langmuir 1997.

The dominance of these hydrolysis reactions yields a very complex chemistry for plutonium even in simple solutions of varying pH and carbonate concentrations. The concentration of the free ion for each oxidation state is plotted as a function of pH for a 10^{-9} molar solution of plutonium Figure 2. Hydrolysis of the Pu^{4+} ion occurs even at very low pH values and and there is very little Pu^{4+} present at a pH slightly greater than one. As the pH increases the hydrolysis of other oxidation states occurs as seen in Figure 2. The effective charge of $Pu(VI)O_2^{2+}$ results in hydrolysis at a pH around 4. This is at a lower pH than Pu(III), which has a smaller effective charge as discussed above. Geochemist Workbench® was used to make the plots in Figure 2 employing the LLNL thermodynamic database (Delany and Lundeen, 1990) and the oxidation state was not allowed to change during the computation.

The extensive hydrolysis of Pu(IV) at low pH values continues until the neutral species $Pu(OH)_4$ is formed (Figure 3) At a pH around 4.5, greater than 50% of the plutonium present is $Pu(OH)_4$, which rises to greater than 99.99% around pH 7. Therefore, when performing experiments within natural pH ranges, hydrolysis reactions lead researchers to deal with $Pu(OH)_2^{+2}$, $Pu(OH)_3^{+}$, and $Pu(OH)_4$ instead of the free Pu^{4+} ion. The formation of $Pu(OH)_4$ also limits the solubility of Pu(IV) species. At Pu(IV) concentrations greater than 10^{-7} *M*, $Pu(OH)_4$(s) precipitates as an amorphous hydroxide polymer that can be separated by ultra-filtration techniques. The amorphous polymer has been shown to form real or intrinsic colloids that

significantly affect its mobility (Nelson, 1987). These aggregates eventually lose a water molecule and form the PuO_2 crystalline solid that is considered to be the thermodynamically stable form of plutonium (Cleveland, 1979).

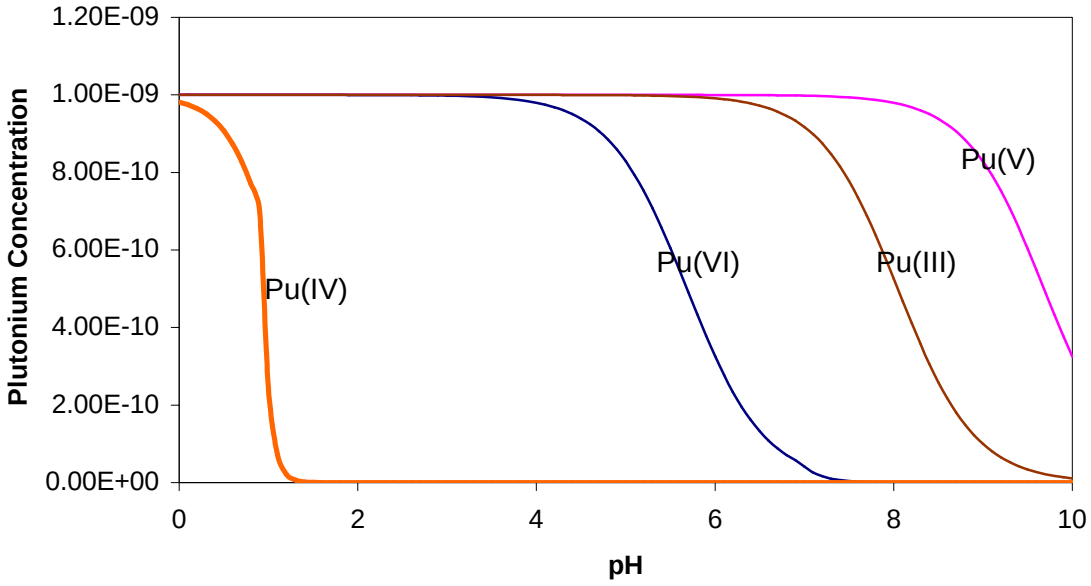

Figure 2. Free ion activity diagram for plutonium oxidation states (Geochemist Workbench LLNL Thermodynamic Constant Database; Delany et al., 1990).

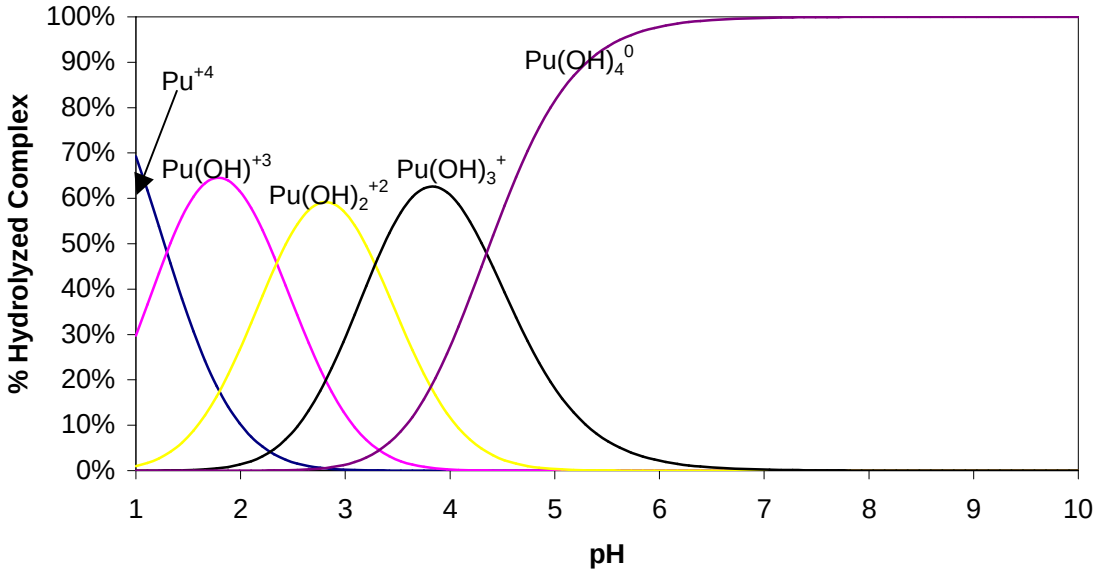

Figure 3. Pu(IV) hydrolysis versus pH (Geochemist Workbench LLNL Thermodynamic Constant Database; Delany et al., 1990).

2.1.3 Solubility

The aqueous phase concentration of plutonium is usually controlled by the presence of $Pu(OH)_4(s)$ or PuO_2 because of the extremely low solubility of these compounds. $Pu(OH)_4(s)$ has pK_{sp} of -56 in a solution at pH 8 with no complexants (Choppin, 1997). The reported pK_{sp} values for PuO_2 range from –54.8 to –57.4 (Neck and Kim, 2001). The similar solubilities stem from the fact that PuO_2 is produced from $Pu(OH)_4(s)$. At concentrations of plutonium high enough to cause homogenous precipitation of polymeric plutonium hydroxide or oxy-hydroxide species colloidal forms of plutonium are produced via aggregation of $Pu(OH)_4(s)$ or $PuO_2(s)$ (Kim 1986). These colloidal forms of plutonium must be separated from the aqueous phase in order to differentiate between aqueous and solid plutonium phases. Approximately 66% of the plutonium polymer can be smaller than 100nm and 0.5% is less than 4.1nm (Nitsche and Edelstein, 1985; Nitsche et al., 1988). Without nano-scale separation methods, plutonium may appear to be more soluble while actually being present in a colloidal form. Some of the colloidal material can be present in aggregates greater than 4.1nm. Therefore, a working knowledge of the nature of colloidal material is needed to define the proper aqueous and solid phases. Kim (1986) reviewed a good example of this phenomenon. Calculations showed that theoretical estimations of PuO_2 solubility based upon the solubility product constant yielded concentrations of plutonium that were 5 orders of magnitude lower than experimental observations. This indicates that thermodynamic data cannot be used to describe plutonium solubility because the constants cannot account for colloid formation.

2.2 PLUTONIUM SORPTION TO NATURAL AND SYNTHETIC MATERIAL

Sanchez et al. (1985) and Keeney-Kennicutt and Morse (1985) studied the sorption of plutonium to natural and synthetic material. Although thermodynamic calculations indicate the Pu(V) is stable under most environmental conditions, interactions with various sorptive surfaces with different redox potentials complicate plutonium sorption characteristics by either oxidizing or reducing the sorbed species.

2.2.1 Pu Interactions with Goethite (α-FeOOH)

Sanchez et al. (1985) preformed sorption experiments with Pu(IV) and Pu(V) on goethite (α-FeOOH). The pH edge (the point at which 50% sorption occurs) for Pu(IV) occurred between pH 3 and 5 and that for Pu(V) was between 5 and 7. However, the Pu(V) edge shifted to a lower pH with time and began to resemble Pu(IV). One explanation for this shift in the sorption edge is that Pu(V) was being reduced to Pu(IV). This reduction was indicated by an experimentally defined solvent extraction technique (Sanchez et al. 1985). Keeney-Kennicutt and Morse (1985) also studied Pu(V) sorption to goethite along with several other natural minerals. Their data suggested that goethite could reduce Pu(V) to Pu(IV). It was also postulated that the reduction could be photochemically catalyzed (Keeney-Kennicutt and Morse, 1985).

The species distribution shown in Figure 2 and Figure 3 indicates that primarily cationic or neutral species of Pu(IV) and Pu(V) are present at the pH values used in these two studies.

Also, at the indicated pH levels the surface of goethite has a net positive charge. As sorption occurred in all studies, it must be inferred that a cationic plutonium species was interacting strongly with a surface containing a positive charge. This type of interaction is in contrast to electrostatic interaction models. Sorption of some cationic species could be the result of interactions with a permanent negative charge present from imperfections and substitutions to the goethite surface but it is not likely that this is the case for all sorption.

2.2.2 Pu Interactions with Manganese Oxides

Interactions of plutonium with manganese oxy/hydroxides are not well understood. The redox chemistry of plutonium varies with respect to the manganese mineral analyzed (Shaugnessy, 2000; Keeney-Kennicutt and Morse, 1985; Duff et al., 1999; Morgenstern and Choppin, 2002). There is an apparent relationship between the manganese oxidation state and its ability to reduce or oxidize plutonium. Minerals containing Mn(II) and Mn(III) oxidation states such as manganite ($Mn(III)O_2H$) and hausmannite ($Mn(II/III)_3O_4$) appear to reduce plutonium (Shaugnessy, 2000). Manganese(IV) minerals such as pyrolusite (β-$Mn(IV)O_2$) and birnessite (δ-$Mn(IV)O_2$) appear to oxidize plutonium (Morgenstern and Choppin, 2002; Keeney-Kennicutt and Morse, 1985). Further work examining the influence of manganese on the speciation of plutonium is needed.

2.2.3 Previous Work with Pu(V) and SRS Burial Ground Sediment

Batch and column studies were preformed by Serkiz et al. (2003) using Pu(V) in SRS Burial Ground sediment. The conceptual model described in the Introduction section includes the reduction of plutonium by iron oxides to explain experimentally observed data. The batch experiments from this study at pH 3, 5, and 8 showed an initial rapid decline in aqueous plutonium concentrations followed by a slower decline that did not reach equilibrium within 3 days. The degree of sorption increased with pH in accordance with pH dependence for the sorption of metal cations to metal oxide surfaces.

In column experiments conducted by Serkiz et al. (2003), both the fractional recovery and the elution time of the major peak, were dependant on pH. The recoveries at pH 3, 5, and 8 were 90%, 75% and 38%, respectively. Retardation factors were 1.4, 8.4, and 35 at pH 3, 5, and 8, respectively. The change in retardation factor was attributed to increased sorption of plutonium; as the pH increased the surfaces developed a large pH-dependant negative charge. The decrease in recovery with increasing pH was attributed to the reduction of Pu(V) to Pu(IV) within the column. In the conceptual model, this would occur because the longer retention times increased the contact time between Pu(V) and the reactive surfaces.

Oxidation state analysis showed that the column influent and effluent was predominantly Pu(V). However, there was a small shoulder that appeared after the main peak for the pH 3 column experiment, suggesting the existence of multiple plutonium species. It was proposed that this small peak could be Pu(IV) (produced either from reduction in the column or present in the spike). However, the sample volumes and concentrations were too small to allow determination of the oxidation state.

Fjeld et al. (2003) incorporated a reduction rate constant into a subsurface transport model for the data of Serkiz et al. (2003). The model fit provided rate constants of $2.0x10^{-4}$, $3.0x10^{-5}$, and $1.3x10^{-5}$ s^{-1} for pH 3, 5, and 8 respectively. These compared well with those of other researchers. The rate constants calculated from the data of Serkiz et al. (2003) ranged from $1.2x10^{-5}$ to $1.4x10^{-5}$ s^{-1} for the 3 pH values investigated and appeared to be independent of pH. Sanchez et al. (1985) calculated reduction rate constants that ranged from $2x10^{-4}$ to $2x10^{-5}$ s^{-1}.

2.3 OBJECTIVES

To gain an understanding of the mobility of different forms of plutonium at the SRS Burial Ground, column and batch sorption edge experiments were conducted with Pu(V) and Pu(IV). All experiments were preformed using 0.02*M* $NaClO_4$ solutions prepared with low-CO_2 distilled-deionized (DDI) water. Pu(V) was chosen in the experiments because it is the least likely Pu oxidation state to form complexes and because it is the predominant oxidation state in natural systems. Along with the non-complexing behavior of the ClO_4^- ion and lack of dissolved inorganic carbon, the chemical conditions should simplify the system so that the environment created will indicate only hydrolysis interactions and interactions between the plutonium and the solid phase. The sediments used in these experiments are described in Table 2. These sediments were selected to represent end-members with respect to sediment properties existing on the SRS that are likely to influence plutonium sorption.

Table 2. SRS sediments used in study.

Name	ID	Description	Sand/Silt/Clay (wt-%)	Surface Area (m^2/g)	pH	Organic Matter (wt-%)
Subsurface Sandy	SubS	Subsurface Yellow Sandy Sediment Low Organic Matter	97/2/1	1.27	5.10	<0.01
Subsurface Clayey	SubC	Subsurface Red Clayey Burial Ground Sediment Low Organic Matter	58/30/12	15.31	4.55	NA
Surface Sandy	SS	Surface Sandy Burial Ground Sediment Clay/Silt, Low Organic Matter	93/6/1	1.37	4.70	<0.01
Surface Clayey	SC	Surface Clayey Forest Sediment High Organic Matter	67/25/8	9.24	5.83	3.2

[(a)] Sand/Silt/Clay was measured by the sieve and pipet method; surface area by the BET N_2 sorption method; pH by the 1:1 sediment:water method; and organic matter by the dry combustion method (Sparks 1996).

3.0 METHODS AND MATERIALS

3.1 COLUMN EXPERIMENTS

3.1.1 Analyses

The experiments were conducted with ^{239}Pu purchased from Isotope Products (Valencia, CA) as a 5μCi/mL stock solution in 4*M* HNO_3. Analyses of all ^{239}Pu solutions were preformed on 1.0mL samples with an alpha-beta discriminating liquid scintillation counter (Wallac Inc., Model 1415). The column experimental apparatus consisted of reservoirs for the plutonium spike and influent solution, a polyvinylchloride column (8.5cm x 1.5cm ID), a peristaltic pump (Masterflex, model 7720-60), and a fraction collector (Eldex Universal Fraction Collector) (Fjeld et al., 2000). Columns were incrementally packed with 2 to 3g aliquots of subsurface sandy sediment at a time and compacted by lightly tapping the base of the column on the desktop. The physical properties of each column are shown in Table 3. The influent solutions were low-carbonate 0.02*M* $NaClO_4$ at pH 3 and pH 5 prepared as described in Serkiz et al. (2003). Perchlorate was chosen as the backing electrolyte because of its low complexation affinity for plutonium. The pH adjusted $NaClO_4$ solution was pumped through the column for 4 - 7 days to reach hydrodynamic equilibrium and to chemically condition the sediment before the plutonium spike was introduced. The weight of the column was monitored until a constant weight was achieved, indicating hydrodynamic equilibrium with all of the available pore spaces filled.

Table 3. Physical properties of packed columns

Column	Pore Volume (mL)	Bulk Soil Density (g/cm^3)	Porosity
pH 3 A	4.36	1.62	0.17
pH 3 B	4.66	1.62	0.19
pH 5 A	4.97	1.62	0.19
pH 5 B	4.81	1.62	0.21
Pu(IV) pH 3	5.02	1.62	0.20

Oxidation state analyses were preformed using an extraction technique adapted from the thenoyltrifluoroacetone (TTA)/di(2-ethylhexyl)orthophosphoric acid (HDEHP) extraction technique discussed by Neu et al. (1994) as well as an ion chromatography (IC) technique (Coates et al., 2001). Two techniques were utilized because of the uncertainty inherent in each method. Oxidation state analyses were preformed on a limited number of samples of the column effluents. As the effluent concentration of plutonium decreased, oxidation state analysis was not possible due to detection limits of the techniques.

3.1.2 Spike Preparation

Plutonium in the pentavalent oxidation state was prepared by the method of Satio et al. (1985) at concentrations from 229 to 309 Bq/mL (4.17 to 5.62 x 10^{-7} *M*). A new spiking solution

was prepared for each column experiment. One column experiment was preformed with Pu(IV) at pH 3 to determine the nature of Pu(IV) transport. The Pu(IV) samples were prepared by adding an aliquot of plutonium stock to a Teflon beaker, evaporating the sample to dryness and dissolving the dried residue in 1.0*M* HNO_3. This process was repeated twice and the final sample residue was dissolved in 0.02*M* $NaClO_4$ at pH 3. Oxidation state analysis was preformed on all spike solutions.

The pH of the spike solution was adjusted with 0.1*M* HNO_3 and measured with an ORION pH Triode Electrode (Beverly, MA). The pH of the spike solution varied from the eluant solution in some columns. Replicate experiments were conducted for each pH (denoted as A and B). The pH was monitored with Broadley-James Microflow pH sensors (Irvine, CA). Tritium, a non-reactive tracer, was added to the spike solution to a final concentration of 7.6 - 17.6 Bq/mL. There was a slight contamination of ^{241}Pu in the plutonium spike that caused some interference with ^{3}H counting due to the similar beta energy of the two nuclides. The contribution of ^{241}Pu was subtracted from the total beta counts observed to determine the ^{3}H activity. This correction was only utilized for pH 3 columns where the effluent front of plutonium overlapped with the ^{3}H tail.

3.1.3 Column Experiment Protocol

The influent was pumped upward through the column at a flow rate of 0.3mL/min. A $^{239}Pu(V)$ spike was introduced as a finite step of approximately one pore volume. The total volume injected was measured by weighing the spike solution before and after the spike. The pH 3 columns were eluted with 70 to 100 pore volumes and the pH 5 columns were eluted with 232 to 250 pore volumes. After spiking, the first 20 to 30 pore volumes were collected in 3.5mL fractions. A 1.0-mL sample from each fraction was removed for liquid scintillation counting and the remainder was used for oxidation state analysis. In some cases the fractions from two adjacent samples were combined to have a sufficient volume for both oxidation state analysis techniques. Also, on selected fractions, samples were filtered through Microsep 30K Centrifugal Filters (estimated effective pore size = 12nm). In these cases 1.0mL was filtered and a 0.5mL aliquot of the filtrate was removed for analysis.

After effluent flow was stopped, the columns were immediately removed and divided into approximately 1cm segments. Each 1cm segment was weighed to determine the packing density of the wet sediment. The plutonium was extracted for 14 days in a solution containing 3.0mL 5*M* HNO_3 and 3.0mL 5*M* HCl. After extraction, a 1.0mL aliquot of each solution was centrifuged, filtered, and a 1.0mL sample was counted by liquid scintillation to determine the extractable activity associated with each segment.

For data analysis, the aqueous concentration in the column effluent were normalized to the spike concentration and plotted as a function of displaced pore volume (DPV). Retardation factors were calculated for both ^{3}H and ^{239}Pu using Equations 3 and 4 below (Clark, 1996).

$$\bar{t} = \frac{\int tC(t)dt}{\int C(t)dt} \quad (3)$$

where $\bar{t}$ is mean residence time in the column. Equation 3 can be expressed in terms of aqueous volume (equation 4).

$$\bar{V} = \frac{\int VC(t)dV}{\int C(t)dV} - \frac{V_{spike}}{2} \quad (4)$$

In equation 4, V is the total volume passed through the column, C(t) is the concentration at time t, and T is the volume of the finite step spike. The retardation factor is calculated by dividing $\bar{V}$ by the pore volume of the column.

3.2 SORPTION EDGE EXPERIMENTS

Separate sorption edges (sorption as a function of pH) were generated for Pu(IV) and Pu(V) for the four sediments listed in Table 2. Each sample was prepared by adding 0.5g of sediment to a pre-weighed, acid washed polypropylene 15mL centrifuge tube (Falcon Blue Max Jr., Becton Dickinson Labware, Franklin Lakes, NJ). The samples were weighed again and the total mass of sediment was determined by difference. Solutions of low CO_2, $NaClO_4$ at various pH values were prepared by adding different aliquots of 0.1M HCl, 0.1M NaOH, 0.04M $NaClO_4$, and DDI H_2O to achieve a final ionic strength of 0.02 within the pH range from 2-10. A 10mL aliquot of these solutions was added to the respective tubes. The tubes were weighed again and the total volume of solution was calculated by difference. The samples were then placed on an end-over-end shaker and pH adjusted every other day with HNO_3 or NaOH until the pH remained stable over the range desired. Samples containing no soil were also prepared to evaluate sorption of the plutonium to the vial walls. Tubes containing sediment but no plutonium spike were run in parallel to perform chemical analysis of the aqueous phase. Results of these analyses are presented in Appendix A.

After the pH remained stable for 48 hours (± 0.1 pH units), Pu(V) and Pu(IV) spikes were prepared as described above. For Pu(V) samples, 0.125mL of a 1547Bq/mL spike was added for a final concentration of approximately 15 Bq/mL. A 0.1mL aliquot of a 2100 Bq/mL Pu(IV) solution was added to each tube to give a final concentration of approximately 21 Bq/mL. Oxidation state analysis was preformed on each spike using the methods discussed above, verifying that greater then 95% of the plutonium was in desired oxidation state. The samples were placed on the shaker for 24 hours, removed, and centrifuged 5 minutes at 5000 RPM. The aqueous phase was then filtered with Microsep 30K centrifugal filters. These filtered are calculated to retain 99% of the particles greater than 12nm. A 1.0mL aliquot of the filtrate was removed for liquid scintillation counting.

The samples containing Pu(IV) and no sediments showed extensive sorption to the vial walls. Therefore, the vials holding the Pu(IV)-sediment samples were immediately analyzed for the sorption to the vial walls. Three 5mL aliquots of DDI water were used to wash out the sediment and aqueous phase from each tube. Then 10mL of 1.0*M* HNO_3 was added to each tube, the tubes were weighed, and then were shaken overnight. A 1.0mL aliquot of each acid solution was removed to determine the total plutonium sorbed to the vial walls. Between 0 and 17% Pu(IV) sorbed to the vial walls for samples containing sediment. The initial concentration was adjusted by this fraction. There was no significant sorption of Pu(V) to the vial walls for the blank samples.

Analysis for iron and total organic carbon was preformed on blank sediment samples containing no plutonium. A Perkin Elmer 5100 Atomic Absorption Spectrophotometer was used for iron determination and a Shimadzu 550 TOC Analyzer was used for organic carbon. Analyses were conducted on filtered and unfiltered samples.

4.0 RESULTS AND DISCUSSION

4.1 COLUMN EXPERIMENTS

4.1.1 Pu(V) Column Analysis

The ^{3}H elution profile for each column experiment are shown in Figure 4 and Figure 5. The curves indicate a single tritium peak that elutes around one DPV. The calculated retardation factors are listed in Table 4. All columns had calculated retardation factor for tritium of either 1.0 or 1.1. This suggests that no "channeling" or preferential flow was occurring within the column.

Measurements of the effluent pH versus DPV are plotted in Figure 6 for all column experiments. Each column was equilibrated with the aqueous phase at the respective pH as described previously. Therefore the small increases in the pH of the effluent observed for the pH3 and pH5 columns are due to the spike. Column pH3-B showed the greater increase in pH due the spike.

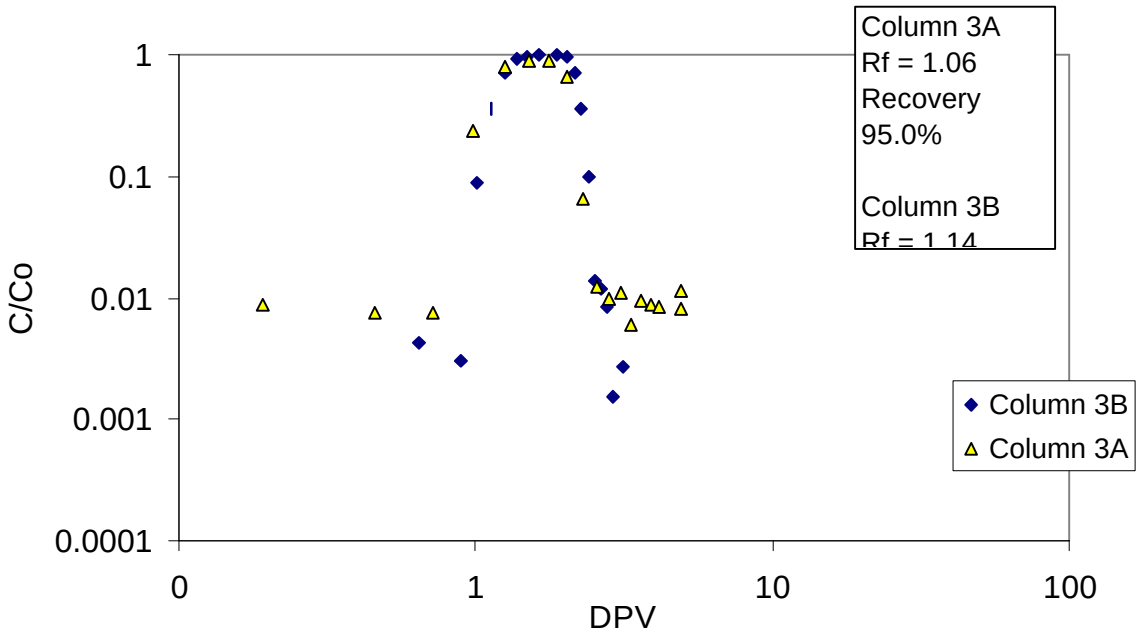

Figure 4. ^{3}H aqueous phase activity profile for pH 3 column experiments (C = concentration, C_o = initial concentration; DPV = displaced pore volumes; Rf = retardation factor).

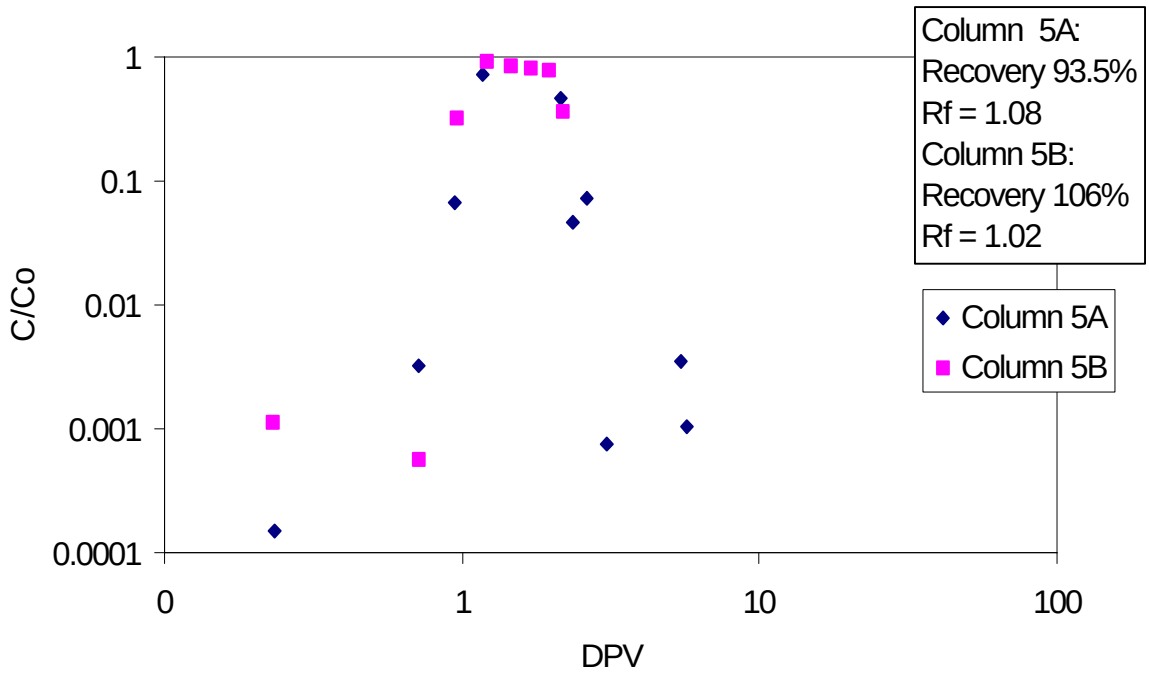

Figure 5. ^{3}H aqueous phase activity profile for pH 5 column experiments (C = concentration, C_o = initial concentration; DPV = displaced pore volumes; Rf = retardation factor).

Table 4. ^{3}H and ^{239}Pu retardation and recovery in pH 3 and pH 5 columns.

Column	^{239}Pu Spike Conc. (Bq/mL)	Displaced Pore Volumes (DPV)	^{3}H Retarda-tion Factor	^{239}Pu Retarda-tion Factor	Aqueous Recovery	Solid-Phase Recovery	Total Recovery
Pu(V) pH 3-A	309.6	71	1.1	1.3	94.1%	1.0%	95.1%
Pu(V) pH 3-B	234	111	1.1	1.9	93.1%	1.4%	94.5%
Pu(V) pH 5-A	229.7	232	1.1	4.4	75.5%	6.5%	82.0%
Pu(V) pH 5-B	280.9	312	1.0	4.8	80.5%	13.3%	93.8%
Pu(IV) pH 3	268.5	1131	1.1	NA	1.7%	64.5%	66.2%

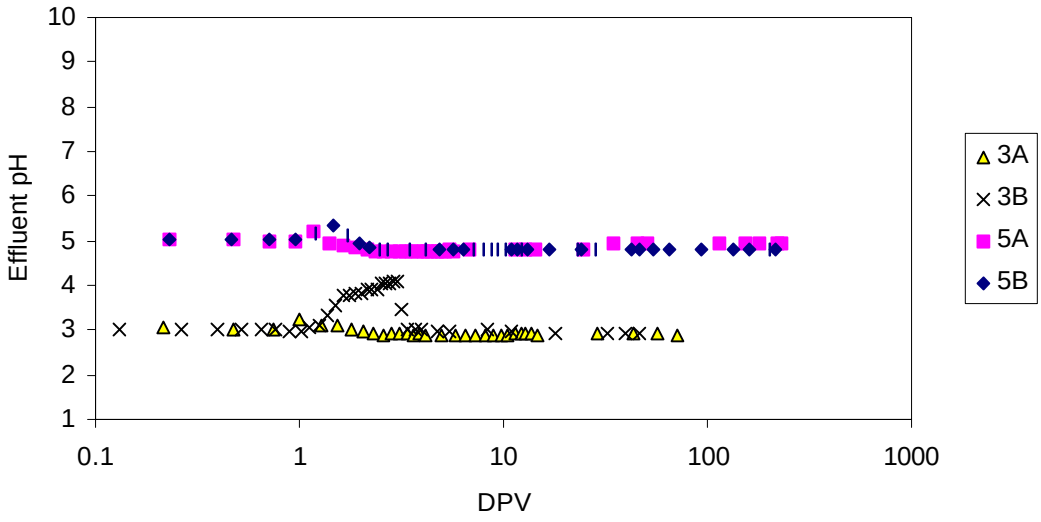

Pu(V) pH 3 and pH 5 column experiments

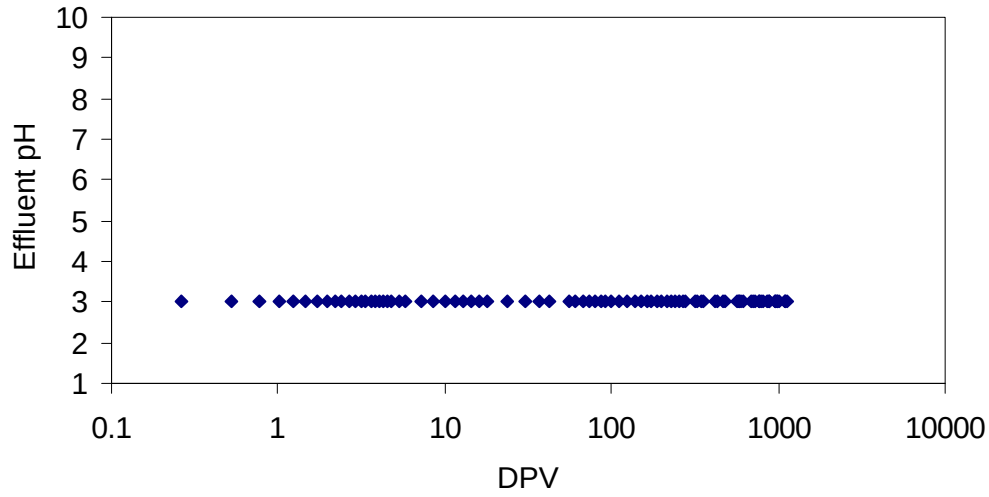

Pu(IV) Column Experiment

Figure 6. Aqueous phase pH profile for plutonium column experiments (DPV = displaced pore volumes; 3A = pH 3 replicate A, 3B = pH 3 replicate B, 5A = pH 5 replicate A, and 5B = pH 5 replicated B).

The aqueous phase activity profiles for Pu(V) column experiments at pH 3 are presented in Figure 7. Total DPVs, spike concentrations, retardation factors, and recoveries for each column are shown in Table 4. The effluent profiles for experiments at pH 3 are characterized by one major peak in the effluent. This is consistent with Pu(V) being present only as the PuO_2^+ cation as suggested in Figure 2. There was little retardation of the main peak at pH3 as the retardation factors were 1.3 and 1.9 for experiment A and B, respectively. The difference in retardation factor between column 3A and 3B was likely attributed to the differences in pH noted above. The aqueous phase recoveries from the experiments were 94.1% and 93.1%, with only an additional ~1% of the Pu recovered from the sediment. **Error! Reference source not found.** contains the oxidation state analyses of the spike solution used for each experiment. According to the ion chromatography (IC) Pu oxidation states analyses, the pH 3 spikes were 3 to 6% Pu(IV). Thus, it is possible that the recoveries of Pu(V) were close to 100%.

Table 5. Plutonium oxidation state analysis results for plutonium column experiments.

Column	Technique	Description/ DPV	Oxidation State Distribution				Avg Recovery
			III	IV	V	VI	
pH 3-A	HEDHP	Spike	0%	1%	82%	17%	*100%
	IC	Spike	6%		97%		107%
	IC	1.5	3%		94%		107%
	IC	2.8	5%		95%		101%
pH 3-B	HEDHP	Spike	0%	1%	85%	13%	*104%
	HEDHP	2.0	1%	0%	76%	22%	*100%
	HEDHP	2.4	0%	1%	87%	13%	*100%
	HEDHP	3.0	0%	1%	85%	15%	*104%
	HEDHP	3.5	1%	2%	80%	18%	*100%
	IC	Spike	4%		96%		110%
	IC	1.4	3%		97%		122%
	IC	1.8	6%		94%		82%
	IC	2.3	13%		87%		93%
	IC	3.5	1%		99%		98%
pH 5-A	HEDHP	Spike	2%	1%	91%	6%	*103%
	HEDHP	3.1	1%	1%	92%	6%	*99%
	HEDHP	3.8	1%	1%	93%	5%	*100%
	HEDHP	4.5	-1%	2%	95%	4%	*106%
	IC	Spike	8%		92%		80%
	IC	2.8	2%		98%		118%
	IC	3.5	12%		88%		112%
	IC	4.7	8%		92%		117%
pH 5-B	HEDHP	Spike	0%	1%	96%	4%	*107%
	HEDHP	3.1	1%	0%	94%	5%	*96%
	HEDHP	4.5	0%	1%	95%	4%	*91%
	HEDHP	6.0	2%	0%	92%	5%	*86%
	HEDHP	7.5	-2%	4%	90%	7%	*107%
	IC	Spike	5%		95%		99%
	IC	3.1	19%		81%		114%
	IC	7.5	7%		93%		120%
Pu(IV) - pH 3	HEDHP	Spike	2%	92%	7%	0%	*92%
	IC	Spike	4%		96%		102%

Notes: The IC (ion chromatography; Section 3.1.1) system can only determine Pu(reduced) and Pu(oxidized). HDEHP: is the organic extraction procedure using TTA & HDEHP discussed in Section 3.1.1

*Average recovery is for the analysis procedure that is a mass balance of 4 samples.

The aqueous phase activity profiles for column experiments 5A and 5B are shown in Figure 8. The retardation factor for Pu(V) increased to approximately 4 as the pH of the aqueous phase was increased to 5 for column experiments 5A and 5B. This increase in retardation factor is consistent with an ion exchange mechanism of plutonium transport in these sediments. As the pH increases, the surface charge of the sediments increases. Therefore, the cationic PuO_2^+ ion is more strongly attracted to the surface, yielding a longer residence time within the column and a higher retardation factor. There was a decrease in the fractional recoveries for both pH5 experiments (Table 4). The observed increase in R and the decrease in fractional recoveries are consistent with previous work with SRS burial ground sediments (Serkiz et al., 2003). Thus, the data is supportive of the ion-exchange and surface-mediated reduction mechanisms within the conceptual model.

The conceptual model reduction of Pu(V) to Pu(IV) within the system introduces the possibility of Pu(IV) partitioning into the aqueous phase. However, these aqueous phase concentrations will be below the current detection limits. A hypothesis including uptake of Pu(IV) that is produced from reduction of Pu(V) explains the lost in fractional recovery of the plutonium spike. Filtration analysis of selected effluent samples indicated that all plutonium contained within the effluent was <12nm, thereby eliminating the possibility of a colloidal plutonium species. Table 6 contains filtration data at selected aqueous effluent fractions. All filtration samples showed greater than 90% recovery of plutonium in the filtrate.

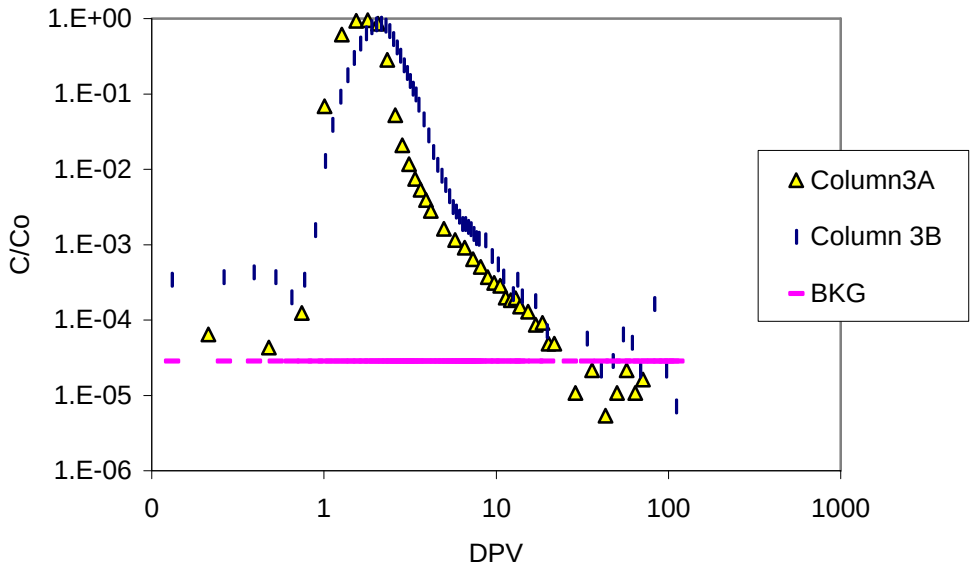

Figure 7. Effluent plutonium activity profile, Pu(V) pH 3 spike column experiments (C = concentration, C_o = initial concentration; DPV = displaced pore volumes; Rf = retardation factor; BFG = background).

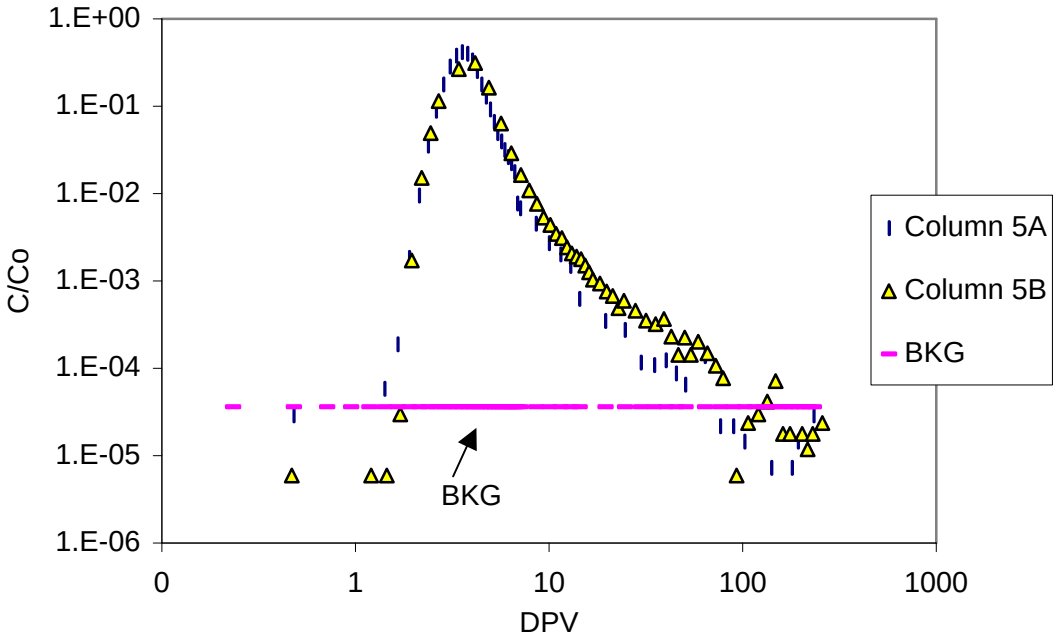

Figure 8. Effluent plutonium activity profile, Pu(V) pH 5 spike column experiments (C = concentration, C_o = initial concentration; DPV = displaced pore volumes; Rf = retardation factor; BFG = background).

The IC oxidation state analyses () indicate that all the spikes for Pu(V) column experiments were approximately 95% Pu(V) and 5% Pu(IV). The variability in the oxidation state analysis methods is partly due to the sensitivity of the methods used as well as the actually oxidation state distribution of plutonium. The recoveries from the techniques were between 80 and 122%, with an average total recovery of 105% ± 12% from 32 experiments, indicating that both techniques performed satisfactorily. Also, there was good agreement between the two techniques. Both indicated that the predominant oxidation state in the effluent from all columns was Pu(V).

If Pu(V) was being reduced to Pu(IV) within the system, followed by Pu(IV) partitioning to the aqueous phase then an increase in Pu(IV) should be seen, though the increase in Pu(IV) concentrations could be below detection limits. An increase in Pu(IV) was not observed in the data (Table 5). Therefore, Pu(V) was the only measured oxidation state in the aqueous phase. Also, the activity of the effluent was all contained in one discrete peak, indicating one plutonium species that is most likely PuO_2^+.

Table 6. Filtration analysis of Pu(V) column experiments.

Column ID	Displaced Pore Volumes (DPV)	Effluent Bq/mL	Filtrate Bq/mL	% Soluble
Column 3A	1.8	209.1	207.3	99%
Column 3A	2.85	23.1	23.1	100%
Column 3B	1.9	68.3	70.4	103%
Column 3B	2.6	98.7	95.1	96%
Column 5A	3.31	86.7	85.4	99%
Column 5A	4.01	76.4	74.3	97%
Column 5B	4.5	66.6	66.5	100%
Column 5B	6.02	13	13.3	102%
Column 5B	7.5	3.81	3.77	99%

At the end of each column test, the sediment was immediately divided into 8 segments and digested with a strong acid solution (5*M* HCl and 5*M* HNO_3) to release plutonium from the sediment. The results (Table 4) indicate that this acid leaching process did not yield a 100% recovery of plutonium from any column experiment. Thus, there appears to be a particularly resistant form of plutonium in the columns that is operationally defined as an "immobile" fraction. In Table 7 are the aqueous, acid soluble, and immobile fractions from all column experiments.

Table 7. Aqueous, acid soluble, and immobile plutonium fractions in pH 3 and pH 5 columns.

Column	Spike Conc. (Bq/mL)	Displaced Pore Volumes (DPV)	Aqueous Fraction [a]	Acid Soluble Fraction [a]	Immobile Fraction [a]
pH 3-A	309.6	71	94.1%	1.0%	4.9%
pH 3-B	234	111	93.1%	1.4%	5.5%
pH 5-A	229.7	232	75.5%	6.5%	18.0%
pH 5-B	280.9	312	80.5%	13.3%	6.2%
Pu(IV) pH 3	268.5	1131	1.7%	64.5%	33.8%

[a] Aqueous Fraction = ^{239}Pu in effluent
Acid Soluble Fraction = ^{239}Pu extracted by 5*M* HNO_3/HCl
Immobile Fraction = 100 – Acid Soluble Fraction – Aqueous Fraction

The acid soluble activity is plotted as a function of distance from the column Figure 9 and Figure 10 for pH 3 and pH 5, respectively. Each column shows a similar profile where the largest fraction was retained within the first two centimeters. The activity recovered from the first two centimeters is likely Pu(IV) in the spike solution. The low mobility of Pu(IV) would cause it to be retained near the column inlet. The approximately uniform distribution of activity

in the remainder of the column is consistent with the Pu(V) reduction hypothesis. As Pu(V) moves through the column, a small amount is continuously reduced to Pu(IV) and retained. This conceptualization is illustrated in Figure 11. The sorbed concentration would actually decline with distance from the inlet because the aqueous phase concentration of Pu(V) declines. The extent of the decline depends on the Pu(V) residence time, i.e., as R increases the decline becomes steeper.

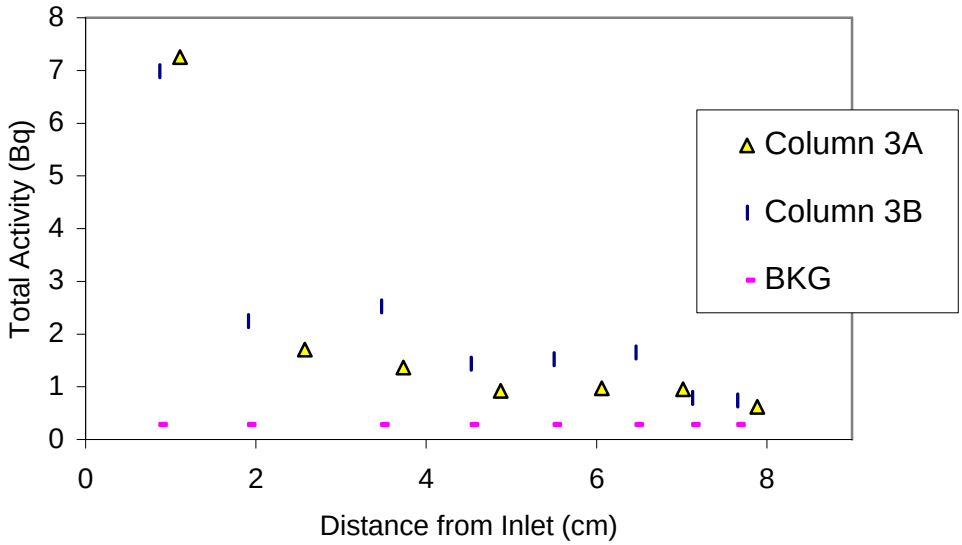

Figure 9. Acid-soluble Pu in sediment as a function of distance in the pH 3 column experiments.

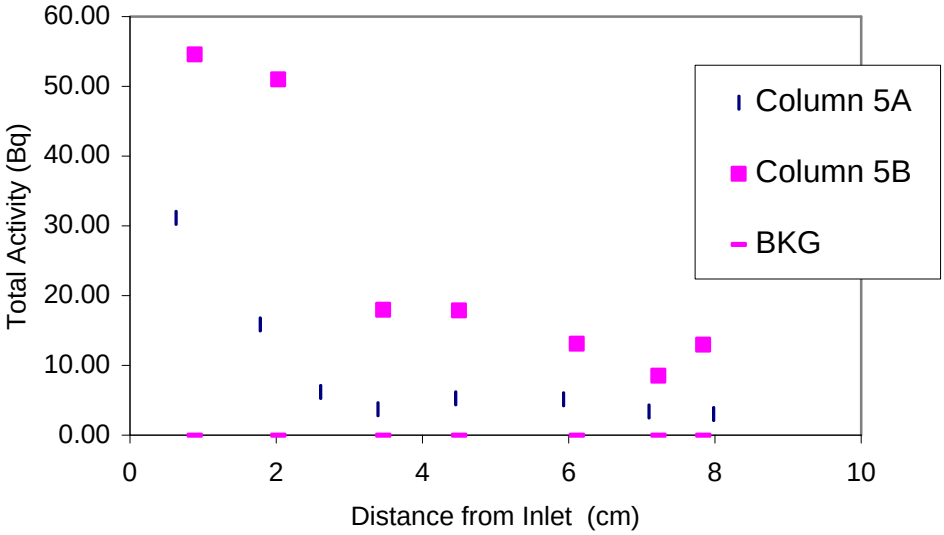

Figure 10. Acid-soluble Pu in sediment as a function of distance in the pH 5 column experiments.

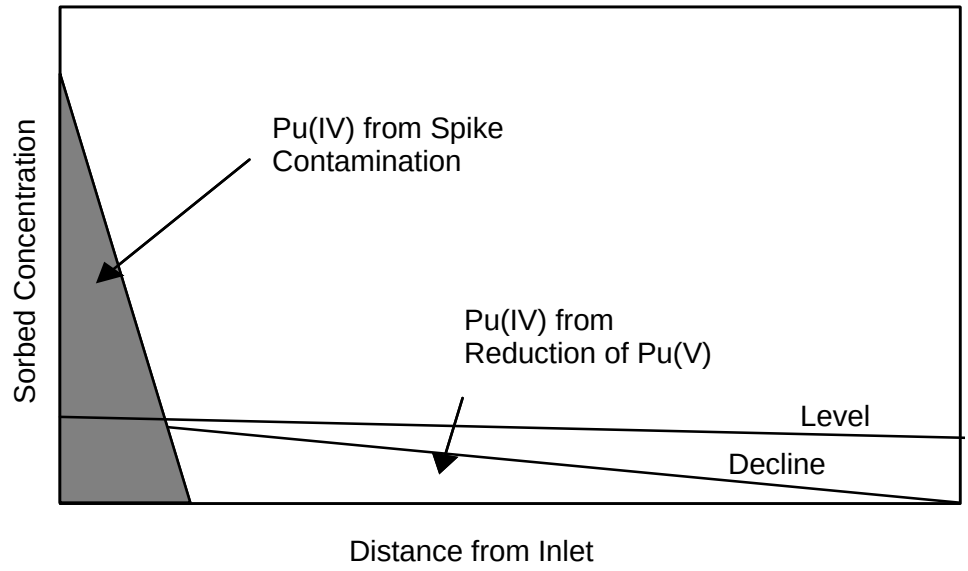

Figure 11. Schematic representation of hypothesis for Pu(IV) source in solid phase activity profiles.

4.1.2 Pu(IV) Column Analysis

One column was spiked with Pu(IV) to determine if aqueous partitioning of sorbed Pu(IV) was likely in this system. There was a small fraction (1.7%) which eluted with ^{3}H, exhibiting no retardation. This was the only aqueous plutonium eluted from the column after 1047 DPV were passed through. Filtration analysis at 12nm verified that this material was a soluble fraction. This may have been due to Pu(V) contamination of the Pu(IV) spike. Oxidation state analyses showed that Pu(V) and Pu(VI) accounted for ~7% of the Pu in the "Pu Table 5). Thus, most, if not all, of the Pu(IV) spiked into solution strongly partitioned to the solid phase and remained associated to the sediment for extended periods of time.

At the end of the experiment, the sediment was digested as done for the Pu(V) column experiments. The solid phase activity profile is shown in Figure 12 and the recovery and retardation factor data are shown in Table 4. The profile differed from those obtained at the end of Pu(V) experiments. First, a larger fraction of the activity was found past the first 1.5cm of the column. Second, there was a much sharper decline in the activity between 1.5cm and the outlet of the column. It cannot be confirmed from this data if the apparent transport was a kinetic limitation for Pu(IV) given the short residence time in the column or if it represents the slow transport of Pu(IV) through the system. Increases in aqueous phase concentrations of Pu(IV) were not detected within the time scales used in the Pu(V) column experiments. Therefore, confirmation of Pu(IV) mobility in these systems must take place using a solid phase oxidation state analysis technique.

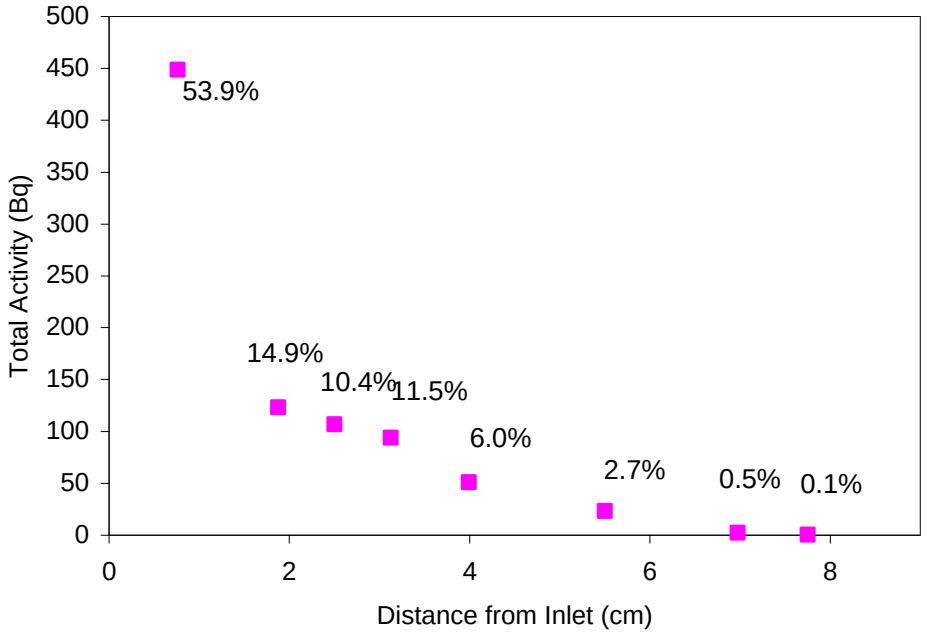

Figure 12. Acid-soluble Pu in sediment as a function of distance in the pH3 Pu(IV) column experiments. Note: Percentages are percent acid-soluble activity.

4.2 SORPTION EDGE EXPERIMENTS

Pu(IV) and Pu(V) sorption edges for all four sediments listed in Table 2 are presented in Figure 13. Overall, the expected trend of strong Pu(IV) sorption is seen for all sediments studied. The sorption edge for Pu(V) shifted with time for all sediments studied, suggesting reduction of Pu(V) to Pu(IV). There are large differences observed between surface and subsurface sediments.

4.2.1 Subsurface Sandy Sediment

For the subsurface sandy sediment approximately 30% sorption of Pu(IV) occurred at pH 1.7 and greater than 95% was sorbed for pH's greater than 2.4. A constant 20% of Pu(V) was sorbed between pH 2 and 5. This sorption of a cationic species at low pH values could be due to a permanent negative charge present on the surface of the sediment from cationic substitutions into the mineral lattice. The speciation distribution in Figure 3 indicates significant amounts of all cationic hydrolysis species of Pu(IV) that could interact with a permanent negative charge on the sediment surface. Around pH 5, Pu(V) sorption increased, until reaching greater than 99% sorption was reached around pH 6.3. After 33 days, the Pu(V) samples were analyzed again and corrected for the new suspended solids concentrations. The sorption edge shifted to a lower pH and the curve began to resemble that of Pu(IV). This behavior is consistent with reduction of Pu(V) to Pu(IV). Oxidation state analysis was performed on the aqueous phase of the lowest pH sample. Pu(V) was still the dominant species, and there was no evidence of Pu(IV) partitioning into the aqueous phase after 33 days.

4.2.2 Subsurface Clayey Sediment

Pu(IV) was more strongly sorbed at low pH values in the subsurface clayey sediment than in the subsurface sandy sediment. There was approximately 80% sorbed at pH 1.7 and greater than 95% sorbed for pH values above 2.3. As seen in the subsurface sandy sediment, the fraction of Pu(V) sorbed was approximately 20% between pH 2 and 4. Between pH 4 and 5.5 the fraction sorbed increased substantially and exceeded 95% at pH 5.5. After 33 days, the plot for Pu(V) was very similar to that for Pu(IV), suggesting reduction of Pu(V).

4.2.3 Surface Sandy Sediment

For the surface sandy sediment, greater than 95% of Pu(IV) was sorbed at pH values greater than 2.3. A small amount of Pu(IV) remained in the aqueous phase at pH 2.0. There is no apparent trend for Pu(V) sorption. The samples were analyzed again after 6 days. During this analysis, one sample was filtered at 12nm and another separate sample was filtered at 3nm. A plot of the Pu(V) sorption edge at 6 days is shown in Figure 14. The sorbed fraction exceeded 93% for all but two samples (pH 1.9 and 4.2). There was no difference between samples filtered at 3nm and 12nm. The smaller size filter was used to ensure that a colloidal form of plutonium was not causing the anomaly observed in the data taken at 24 hours. After 33 days the plot of Pu(V) closely resembled that of Pu(IV).

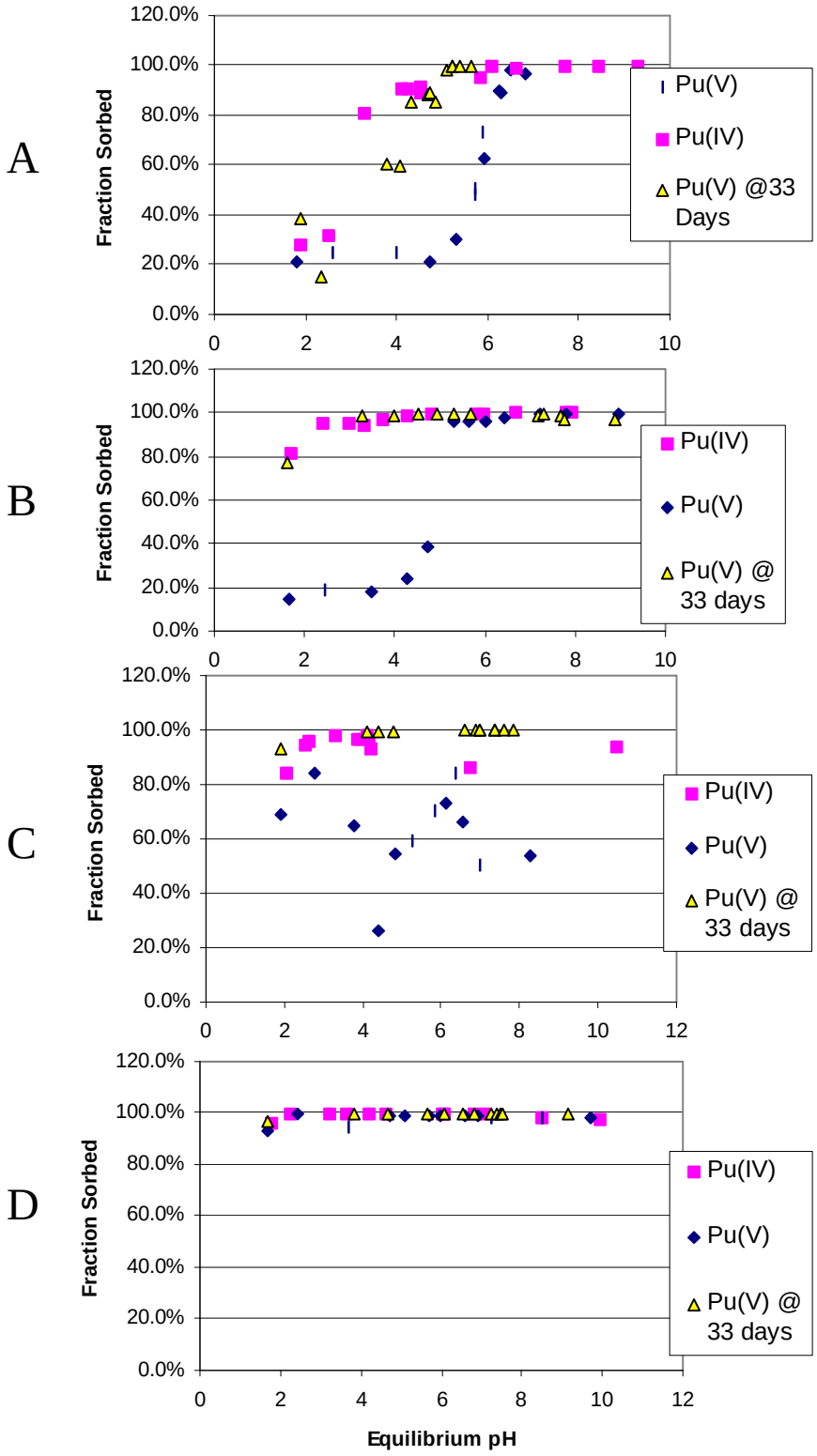

Figure 13. Pu(IV) and Pu(V) sorption edge at 24 hr or 33 days on: (A) subsurface sandy sediment, (B) subsurface clayey sediment, (C) surface sandy sediment, and (D) surface clayey sediment.

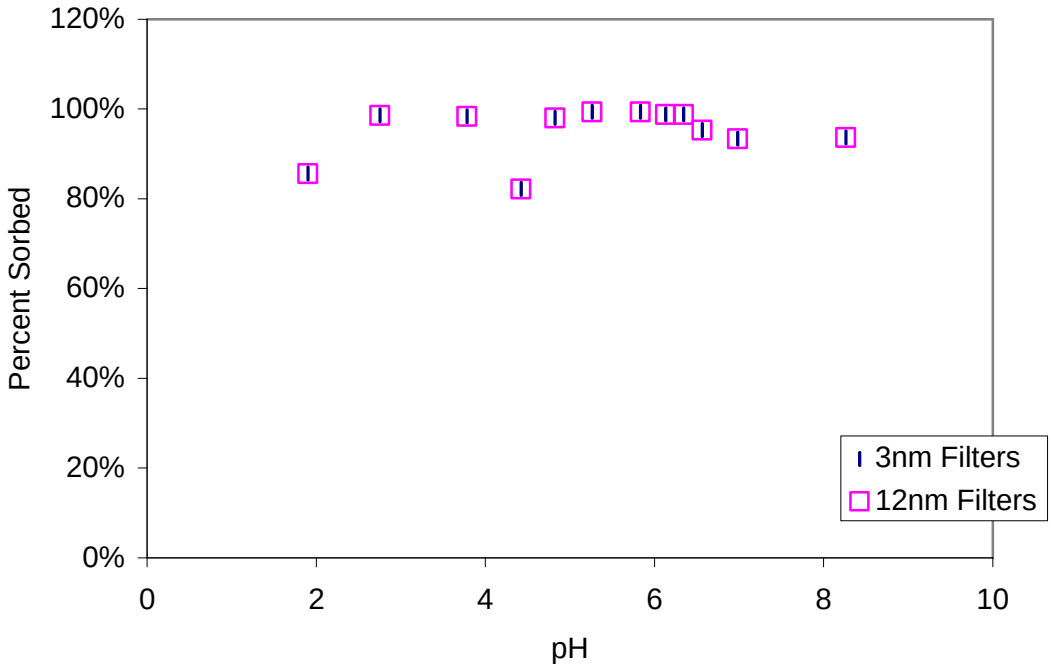

Figure 14. Pu(V) sorption edge on surface sandy sediment at 6 days.

4.2.4 Surface Clayey Sediment

In all cases greater than 95% sorption occurred for both oxidation states in the pH range 1.6 to 9.8 within 24 hours. Data taken at 33 days from the Pu(V) samples show no significant variation from the data taken at 24 hours. Strong sorption to this sediment is likely attributed to the greater surface area and organic matter concentration of this sediment (Table 2).

4.2.5 Calculation of Kd from Sorption Edge Experiments

The "apparent K_d" for each sample is given in Appendix B. The term "apparent K_d" is used for this quantity because the samples may not have reached equilibrium and Pu(IV) colloids less than 12nm may have affected the measurements. Presented in Table 8 are the ranges of "apparent K_d" for each sediment. These values were obtained from:

$$K_d = \frac{C_o - C_t}{C_t} \bullet \frac{1}{SS} \qquad (4)$$

where C_o is the initial plutonium aqueous phase concentration, C_t is the plutonium aqueous phase concentration at time = t, and SS is the suspended solids concentration. Also, the values at the

upper ends of the range, i.e., the larger Kd values, were calculated using aqueous phase concentrations that were close to the detection limit. Consequently, the uncertainty associated with these values is high.

Table 8. Apparent Kd range for sorption edge sediments.

Sediment	Sample Description	Apparent Kd Range
Subsurface Sandy	Pu(IV)	8 to 9300
Subsurface Sandy	Pu(V)	6 to 1100
Subsurface Sandy	Pu(V) at 33 days	3 to 4900
Subsurface Clayey	Pu(IV)	90 to 50000
Subsurface Clayey	Pu(V)	4 to 660
Subsurface Clayey	Pu(V) at 33 days	60 to 10100
Surface Clayey	Pu(IV)	500 to 4600
Surface Clayey	Pu(V)	300 to 2600
Surface Clayey	Pu(V) at 33 days	500 to 33000
Surface Sandy	Pu(IV)	100 to 1100
Surface Sandy	Pu(V)	7 to 100
Surface Sandy	Pu(V) at 33 days	150 to 20000

5.0 SUMMARY

The principal findings of this research are as follows.

Column Experiments

- The retardation factor of $Pu(V)O_2^+$ increased with pH. This is consistent with an ion exchange sorption mechanism. The fractional recovery of $Pu(V)O_2^+$ in the column effluent decreased as the pH of the influent solution increased. These findings are consitent with previous work in SRS sediments and support the hypothesis of an ion-exchange sorption mechanism coupled with surface mediated reduction of Pu(V).

- All four column effluent profiles show one main peak, indicating one plutonium species. This does not agree with a previous single column result conducted with pH3 SRS sediment (Serkiz et al., 2003) in which two peaks were observed in the effluent profile.

- Two separate methods of oxidation state analysis show no evidence of Pu(IV) in column effluents spiked with Pu(V).

- A column spiked with Pu(IV) had no significant aqueous activity eluted within 1000 DPV. The apparent limited mobility of Pu(IV) could be due to a kinetic limitation of sorption or slow transport of Pu(IV) within the column. Further experiments are required to determine the precise mechanism of Pu mobility under these experimental conditions.

- The less than 100% recoveries observed following strong acid leaching for several column experiments indicates that the plutonium may be irreversibly sorbed to the sediment surface or interstitial spaces.

Batch Experiments

- All sorption edge data for Pu(IV) indicates strong sorption for the pH range in this work. Therefore transport of Pu(IV) within a column is not likely.

- The sorption edge of Pu(V) shifted with time to resemble that of Pu(IV) for all sorption edge experiments. This suggests the reduction of Pu(V) to Pu(IV) within these systems.

- Non-zero sorption for Pu(IV) and Pu(V) was observed at low pH values for all sorption edge experiments. Therefore, even at low pHs the cationic plutonium species significantly adsorb to the sediment.

6.0 REFERENCES

Allard, B., Kipatsi, H., Liljenzin, J.O., "Expected Species of Uranium, Neptunium, and Plutonium in Neutral Aqueous Solutions" *J. Inorg. Nucl. Chem.* 42, 1015-1027, 1980.

Choppin, G.R., Bond, A.H., and Hromadka, P.M. "Redox Speciation of Plutonium" *J. of Radio. Nucl. Chem.* 219(2), 203-210, 1997.

Clark, M.M., Transport Modeling for Environmental Engineers and Scientists, John Wiley and Sons, Inc., New York, 1996.

Clevland, J.M. *The Chemistry of Plutonium* p. 651. American Nuclear Society, La Grange Park, Il (1979).

Coates, J.T., Fjeld, R.A., Paulenova, A., and DeVol, T., "Evaluation of a Rapid Technique for Measuring Actinide Oxidation States in a Groundwater Simulant," *J. Radioanal. Nucl. Chem.*, 248(2), 501-506, 2001.

Delany, J.M. and Lundeen, S.R., "The LLNL Thermochemical Database", Lawrence Livermore National Laboratory Report UCRL-21658, 150 p., 1990.

Duff, M.C., Hunter, D.B., Triay, I.R., Bertsch, P.M., Reed, D.T., Sutton, S.R., Shea-McCarthy, G., Kitten, J., Eng, P., Chipera, S.J., and Vaniman, D.T., "Mineral Associations and Average Oxidation States of Sorbed Pu on Tuff" *Environ. Sci. Tech*. 33, 2163-2169, 1999.

Farr J.D., Schulze, R.K., and Honeymann, B.D. "Aqueous Pu(IV) Sorption on Brucite" *Radiochim. Acta.* 88, 675-679, 2000.

Fjeld, R. A., Coates, J. T., and Elzerman, A. W., "Column Tests to Study the Transport of Plutonium and Other Radionuclides in Sedimentary Interbed at INEEL," Final Report submitted to the Idaho National Engineering and Environmental Laboratory, Idaho Falls, ID, December 2000.

Fjeld, R. A., DeVol, T. A., Goff, R. W., Blevins, M. D., Brown, D. D., Ince, S. M., and Elzerman, A. W., "Characterization of Mobilities of Selected Actinides and Fission/Activation Products in Laboratory Columns Containing Basalt and Sedimentary Interbed from the Snake River Plain" *Nuclear Technology*. In press, 2003.

Fjeld, R.A., Serkiz S.M., McGinnis P.L., Elci A., Kaplan D.I., "Evaluation of a Conceptual Model for the Subsurface Transport of Plutonium Involving Surface Mediated Reduction of Pu(V) to Pu(IV)." *J. of Cont. Hydro*. In review, 2003

Haschke, J.M., Allen, T.H., "Equilibrium and thermodynamic Properties of the PuO2+x Solid *J of Alloy and Comp.* 2002, 336, 124-131.

Haschke, J.M., Allen T.H., and L.A. Morales, "Reaction of Plutonium Dioxide With Water: Formation and Properties of PuO_{2+x}", *Science,* Volume 287, pp.285-287, 1/14 (2000).

Hobart, D.E., "Actinides in the Environment" Proceedinigs of The Robert A. Welch Conference on Chemical Research XXXIV Fifty Years with Transuranium Elements." October 22-23, 1990, Houston, TX, 1990.

Keeney-Kennicutt, W.L. and Morse, J.W. "The Redox Chemistry of PuO_2^+ Interaction with Common Mineral Surfaces in Dilute Solutions and Seawater" *Geochim. Cosmochim. Acta*, 49, 2577-2588, 1985.

Kim, J.O. "Chemical Behavior of Transuranic Elements in Natural Aquatic Systems" In A.J. freeman and C. Keller (Eds.) Handbook of the Physics and Chemistry of the Actinides, Volume 4. North-Holland Press, Amsterdam p. 413-455, 1986.

Langmuir, D. *Aqueous Environmental Chemistry,* Prentice Hall, Upper Saddle River, New Jersey, 1997, p. 486-547

Morgenstern, A. and Choppin, G.R., "Kinetics of the Oxidation of Pu(IV) by Manganese Oxide" *Radiochim. Acta*, 90(2), 69-74, 2002.

Neck, V. and Kim, J.I., " Solubility and Hydrolysis of Tetravalent Actinides" *Radiochim. Acta* 88(1), 1-16, 2001.

Nelson, D.M., Larson, R.P., and Penrose, W.R., "Chemical Speciation of Plutonium In Natural *Environmental Research on Actinide Elements*, J.E. Pinder, J.J. Alberts, K.W. McLeod, and R.G. Schreckhise (eds.), p. 27-48, CONF-841142, Office of Scientific and Technical Information, U.S. Department of Energy, Washington D.C., 1987.

Neu, M.P., Hoffman, D.C., Roberts, K.E., Nitsche, H., Silva, R.J., "Comparison of Chemical Extractions and Laser Photoacoustic Spectroscopy for the Determination of Plutonium Species in Near-Neutral Carbonate Solutions" *Radiochim. Acta*, 66, 265-272, 1994.

Nitsche, H., and Edelstein, N.M., "Solubilities and Speciation of Selected Transuranium Ions. A Comparison of a Non-Complexing Solution with a Groundwater from the Nevada Tuff Site" *Radiochim. Acta.*, 39, 23-33, 1985.

Nitsche, H., Lee, S.C., Gatti, R.C., "Determination of Plutonium Oxidation States at Trace Levels Pertinent to Nuclear Waste Disposal" *J. Radioanal. Nucl. Chem.* 124(1), 171-185, 1988.

Prout, W.E. "Adsorption of Fission Products by Savannah River Plant Soil" *Soil Sci.* 13-17, 1958
Sanchez A.L., Murray J.W., and Sibley T.H. "The Adsoption of Plutonium IV and V on *Geochim. et Comochim. Acta*, 49, 2297-2307, 1985.

Satio, A.M., Roberts R.A., and Choppin G.R., "Preparation of Tracer Level Plutonium(V)", *Anal. Chem.* 57, 390-391, 1985.

Serkiz, S. M.,Gibbs, B. W., Fjeld, R. A., and Coates, J. T. "The Influence of pH on Plutonium (V) Transport Through a Sandy Atlantic Coastal Plain Soil in a Low-Carbonate System." In preparation. 2003.

Shaugnessy, D.A., Nitsche, H., Serne, R.J. Shuh, D.K., Waychunas, G.A., Booth, C.H., and Gill, H.S. "Interfacial Reaction Studies of Plutonium on Manganese Oxide Hydroxide Mineral *Abstr. Pap. Am. Chem. Soc.* 220: 227-ENVR Part 1, August 20, 2000.

Silva, R.J. and Nitsche, H. "Actinide Environmental Chemistry" *Radiochim. Acta.* 70/71, 377-396, 1995.

Sparks, D. L. (Editor) 1996. Methods of Soil Analysis, Part 3 – Chemical Methods. Soil Science Society of America Publishers, Madison, WI.

7.0 APPENDIX A: IRON AND ORGANIC CARBON MEASUREMENTS OF SORPTION EDGE BLANK SAMPLES

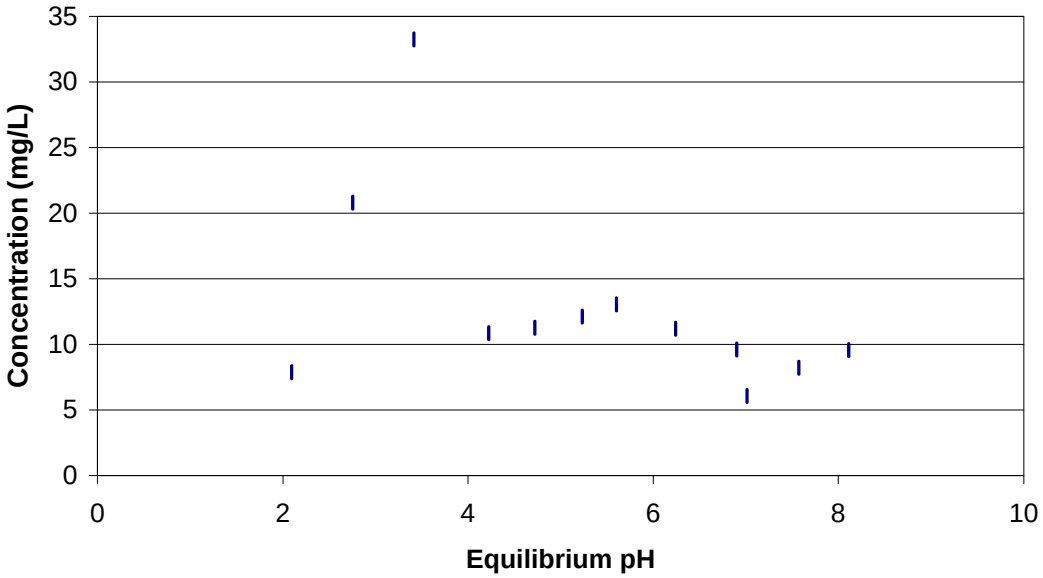

Figure A. 1. TOC versus pH for sorption edge blank samples, subsurface sandy.

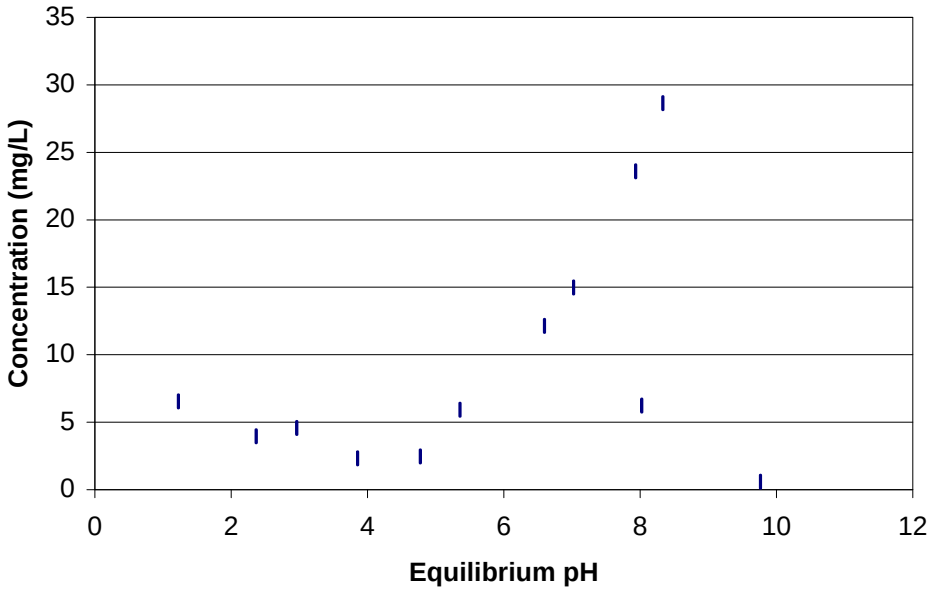

Figure A. 2. TOC versus pH for sorption edge blank samples, subsurface clayey.

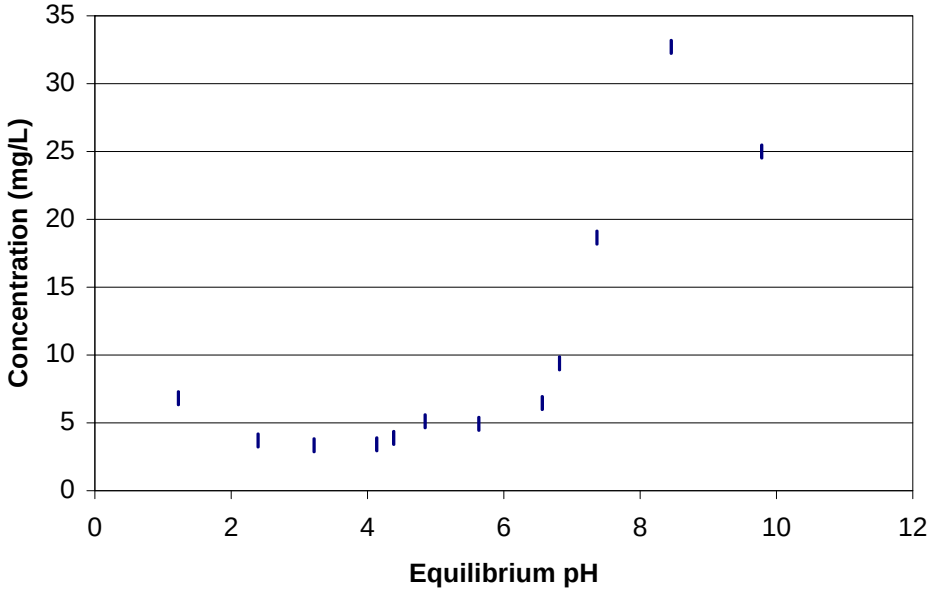

Figure A. 3. TOC versus pH for sorption edge blank samples, surface sandy.

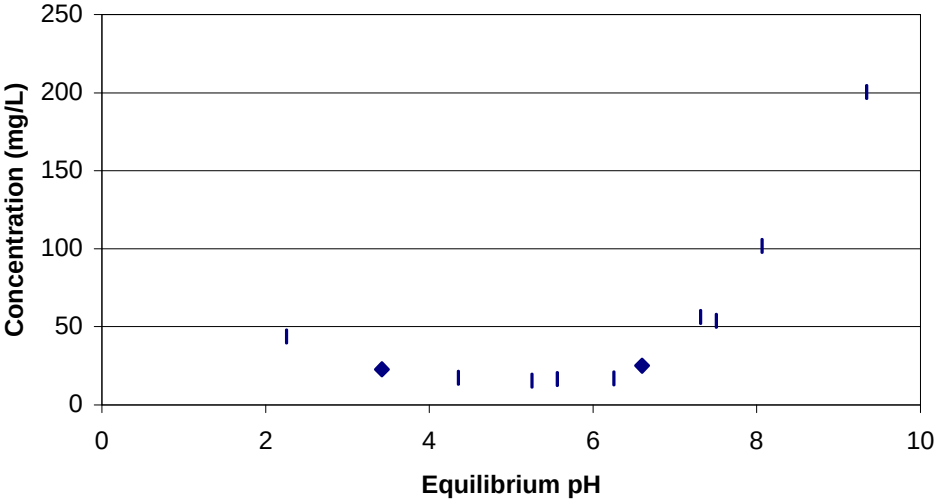

Figure A. 4. TOC versus pH for sorption edge blank samples, surface clayey.

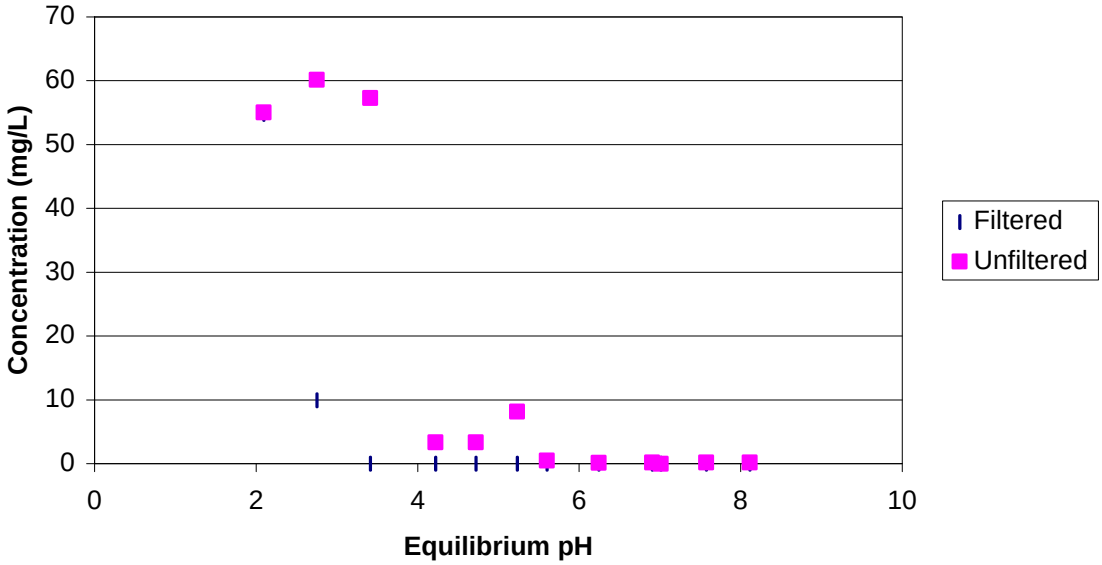

Figure A. 5. Iron determination in sorption edge blanks, subsurface sandy.

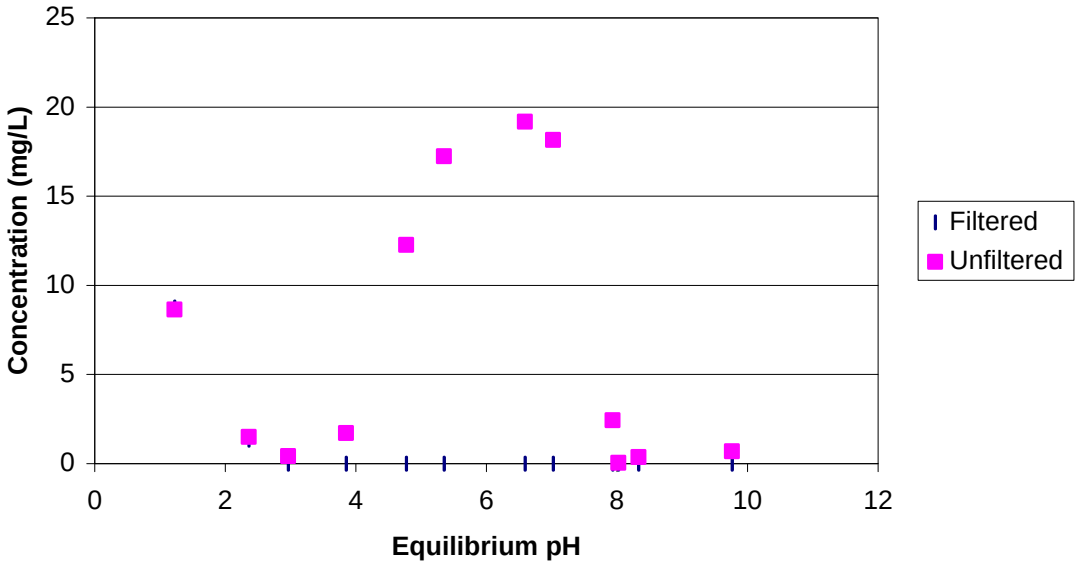

Figure A. 6. Iron determination in sorption edge blanks, subsurface clayey.

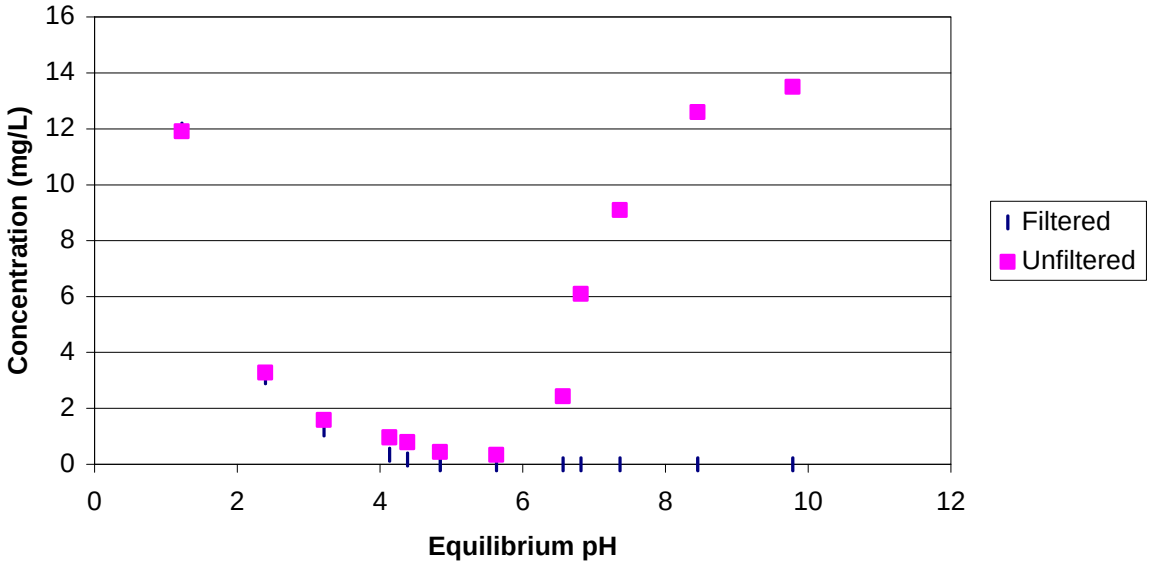

Figure A. 7. Iron determination in sorption edge blanks, Surface Sandy Sediment.

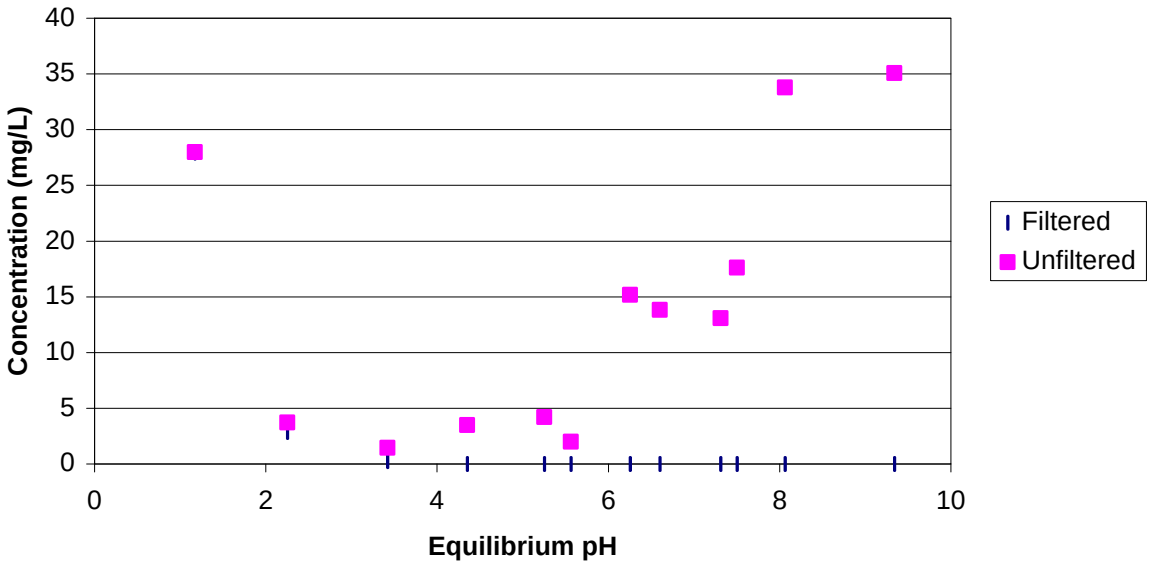

Figure A. 8. Iron determination in sorption edge blanks, Surface Clayey Sediment.

8.0 APPENDIX B: APPARENT KD CALCULATIONS FROM SORPTION EDGE SAMPLES

Table B. 1. Apparent Kd values from plutonium sorption edge experiments.

Sample ID	Sample Description	pH	Apparent Kd
Subsurface Sandy	Pu(IV)	1.91	8
Subsurface Sandy	Pu(IV)	2.52	9
Subsurface Sandy	Pu(IV)	3.29	90
Subsurface Sandy	Pu(IV)	4.12	180
Subsurface Sandy	Pu(IV)	4.51	160
Subsurface Sandy	Pu(IV)	4.23	190
Subsurface Sandy	Pu(IV)	4.53	220
Subsurface Sandy	Pu(IV)	5.85	390
Subsurface Sandy	Pu(IV)	6.61	2500
Subsurface Sandy	Pu(IV)	6.10	2800
Subsurface Sandy	Pu(IV)	7.70	2800
Subsurface Sandy	Pu(IV)	8.42	20000
Subsurface Sandy	Pu(IV)	9.28	9300
Subsurface Sandy	Pu(V)	1.81	6
Subsurface Sandy	Pu(V)	2.58	7
Subsurface Sandy	Pu(V)	3.99	7
Subsurface Sandy	Pu(V)	4.75	6
Subsurface Sandy	Pu(V)	5.30	9
Subsurface Sandy	Pu(V)	5.72	20
Subsurface Sandy	Pu(V)	5.72	20
Subsurface Sandy	Pu(V)	5.94	30
Subsurface Sandy	Pu(V)	5.90	60
Subsurface Sandy	Pu(V)	6.27	180
Subsurface Sandy	Pu(V)	6.28	160
Subsurface Sandy	Pu(V)	6.51	1100
Subsurface Sandy	Pu(V)	6.83	700
Subsurface Sandy	Pu(V) @ 33 days	1.91	10
Subsurface Sandy	Pu(V) @ 33 days	2.36	3
Subsurface Sandy	Pu(V) @ 33 days	3.79	30
Subsurface Sandy	Pu(V) @ 33 days	4.06	30
Subsurface Sandy	Pu(V) @ 33 days	4.32	90
Subsurface Sandy	Pu(V) @ 33 days	4.69	110
Subsurface Sandy	Pu(V) @ 33 days	4.72	130
Subsurface Sandy	Pu(V) @ 33 days	4.87	100
Subsurface Sandy	Pu(V) @ 33 days	5.10	600
Subsurface Sandy	Pu(V) @ 33 days	5.21	4800
Subsurface Sandy	Pu(V) @ 33 days	5.23	3700
Subsurface Sandy	Pu(V) @ 33 days	5.41	4900
Subsurface Sandy	Pu(V) @ 33 days	5.62	3100

Table B. 2. Apparent Kd values from plutonium sorption edge experiments

Sample ID	Sample Description	pH	Apparent Kd
Subsurface Clayey	Pu(IV)	1.71	90
Subsurface Clayey	Pu(IV)	2.39	410
Subsurface Clayey	Pu(IV)	2.98	410
Subsurface Clayey	Pu(IV)	3.34	350
Subsurface Clayey	Pu(IV)	3.74	670
Subsurface Clayey	Pu(IV)	4.26	1300
Subsurface Clayey	Pu(IV)	4.81	2100
Subsurface Clayey	Pu(IV)	5.98	9000
Subsurface Clayey	Pu(IV)	5.82	6600
Subsurface Clayey	Pu(IV)	6.68	18000
Subsurface Clayey	Pu(IV)	7.91	50000
Subsurface Clayey	Pu(IV)	7.79	42000
Subsurface Clayey	Pu(V)	1.67	4
Subsurface Clayey	Pu(V)	2.46	5
Subsurface Clayey	Pu(V)	3.50	4
Subsurface Clayey	Pu(V)	4.27	6
Subsurface Clayey	Pu(V)	4.74	10
Subsurface Clayey	Pu(V)	5.30	50
Subsurface Clayey	Pu(V)	5.63	50
Subsurface Clayey	Pu(V)	6.45	100
Subsurface Clayey	Pu(V)	6.02	440
Subsurface Clayey	Pu(V)	7.24	2300
Subsurface Clayey	Pu(V)	7.82	2600
Subsurface Clayey	Pu(V)	8.95	6600
Subsurface Clayey	Pu(V) @ 33 days	1.63	60
Subsurface Clayey	Pu(V) @ 33 days	3.28	1400
Subsurface Clayey	Pu(V) @ 33 days	4.00	1600
Subsurface Clayey	Pu(V) @ 33 days	4.53	2300
Subsurface Clayey	Pu(V) @ 33 days	4.95	9300
Subsurface Clayey	Pu(V) @ 33 days	5.32	10000
Subsurface Clayey	Pu(V) @ 33 days	5.68	4700
Subsurface Clayey	Pu(V) @ 33 days	7.16	1600
Subsurface Clayey	Pu(V) @ 33 days	7.32	3700
Subsurface Clayey	Pu(V) @ 33 days	7.69	1300
Subsurface Clayey	Pu(V) @ 33 days	7.74	600
Subsurface Clayey	Pu(V) @ 33 days	8.89	540

Table B. 3. Apparent Kd values from plutonium sorption edge experiments

Sample ID	Sample Description	pH	Apparent Kd
Surface Clayey	Pu(IV)	1.78	500
Surface Clayey	Pu(IV)	2.26	3200
Surface Clayey	Pu(IV)	3.21	3200
Surface Clayey	Pu(IV)	3.64	3200
Surface Clayey	Pu(IV)	4.18	4900
Surface Clayey	Pu(IV)	4.63	3000
Surface Clayey	Pu(IV)	6.09	1000
Surface Clayey	Pu(IV)	6.02	4600
Surface Clayey	Pu(IV)	6.83	3700
Surface Clayey	Pu(IV)	7.11	3500
Surface Clayey	Pu(IV)	8.49	1300
Surface Clayey	Pu(IV)	9.95	800
Surface Clayey	Pu(V)	1.68	300
Surface Clayey	Pu(V)	2.44	5600
Surface Clayey	Pu(V)	3.70	330
Surface Clayey	Pu(V)	4.71	2500
Surface Clayey	Pu(V)	5.10	2300
Surface Clayey	Pu(V)	5.68	2400
Surface Clayey	Pu(V)	5.98	2600
Surface Clayey	Pu(V)	6.60	1400
Surface Clayey	Pu(V)	6.89	1300
Surface Clayey	Pu(V)	7.23	1300
Surface Clayey	Pu(V)	8.52	1000
Surface Clayey	Pu(V)	9.69	900
Surface Clayey	Pu(V) @ 33 days	1.68	5100
Surface Clayey	Pu(V) @ 33 days	3.81	3300
Surface Clayey	Pu(V) @ 33 days	4.67	13000
Surface Clayey	Pu(V) @ 33 days	5.67	13000
Surface Clayey	Pu(V) @ 33 days	6.05	13000
Surface Clayey	Pu(V) @ 33 days	6.55	8200
Surface Clayey	Pu(V) @ 33 days	6.81	33000
Surface Clayey	Pu(V) @ 33 days	7.22	8200
Surface Clayey	Pu(V) @ 33 days	7.36	33000
Surface Clayey	Pu(V) @ 33 days	7.49	33000
Surface Clayey	Pu(V) @ 33 days	7.53	13000
Surface Clayey	Pu(V) @ 33 days	9.15	3300

Table B. 4. Apparent Kd values from plutonium sorption edge experiments

Sample ID	Sample Description	pH	Apparent Kd
Surface Sandy	Pu(IV)	2.05	100
Surface Sandy	Pu(IV)	2.51	330
Surface Sandy	Pu(IV)	2.65	130
Surface Sandy	Pu(IV)	3.30	970
Surface Sandy	Pu(IV)	3.88	590
Surface Sandy	Pu(IV)	3.98	530
Surface Sandy	Pu(IV)	4.09	1100
Surface Sandy	Pu(IV)	4.13	860
Surface Sandy	Pu(IV)	4.18	620
Surface Sandy	Pu(IV)	4.19	260
Surface Sandy	Pu(IV)	6.73	130
Surface Sandy	Pu(IV)	10.47	290
Surface Sandy	Pu(V)	1.90	50
Surface Sandy	Pu(V)	2.75	100
Surface Sandy	Pu(V)	3.78	360
Surface Sandy	Pu(V)	4.42	7
Surface Sandy	Pu(V)	4.82	30
Surface Sandy	Pu(V)	5.26	30
Surface Sandy	Pu(V)	5.83	50
Surface Sandy	Pu(V)	6.13	50
Surface Sandy	Pu(V)	6.34	110
Surface Sandy	Pu(V)	6.56	40
Surface Sandy	Pu(V)	6.98	20
Surface Sandy	Pu(V)	8.26	20
Surface Sandy	Pu(V) @ 6 days	1.90	100
Surface Sandy	Pu(V) @ 6 days	2.75	1100
Surface Sandy	Pu(V) @ 6 days	3.78	1700
Surface Sandy	Pu(V) @ 6 days	4.42	60
Surface Sandy	Pu(V) @ 6 days	4.82	510
Surface Sandy	Pu(V) @ 6 days	5.26	2900
Surface Sandy	Pu(V) @ 6 days	5.83	1400
Surface Sandy	Pu(V) @ 6 days	6.13	1800
Surface Sandy	Pu(V) @ 6 days	6.34	1700
Surface Sandy	Pu(V) @ 6 days	6.56	400
Surface Sandy	Pu(V) @ 6 days	6.98	270
Surface Sandy	Pu(V) @ 6 days	8.26	210
Surface Sandy	Pu(V) @ 33 days	1.91	150
Surface Sandy	Pu(V) @ 33 days	4.11	2900

Table B.4 (continuation): Apparent Kd values from plutonium sorption edge experiments

Sample ID	Sample Description	pH	Apparent Kd
Surface Sandy	Pu(V) @ 33 days	4.41	2200
Surface Sandy	Pu(V) @ 33 days	4.78	1200
Surface Sandy	Pu(V) @ 33 days	6.61	8300
Surface Sandy	Pu(V) @ 33 days	6.89	8300
Surface Sandy	Pu(V) @ 33 days	7.00	5700
Surface Sandy	Pu(V) @ 33 days	7.36	20000
Surface Sandy	Pu(V) @ 33 days	7.58	20000
Surface Sandy	Pu(V) @ 33 days	7.86	20000
Surface Sandy	Pu(V) @ 33 days	7.00	20000
Surface Sandy	Pu(V) @ 33 days	7.36	20000